SUN GLARE: NETWORK CHARACTERIZATION AND SAFETY EFFECTS

by

Danyang Sun

A thesis submitted in partial fulfillment of the requirements for the degree of

Master of Science

in

TRANSPORTATION ENGINEERING

Department of Civil and Environmental Engineering
University of Alberta

Abstract

Visibility is one of the basic requirements for safe driving. Any type of vision obstruction can interfere with the driver's ability to operate a vehicle and thus poses a significant risk to road traffic safety. In addition to widely investigated adverse weather conditions such as rain, fog, and snow, which can reduce visibility, bright sunny days may also bring challenges to safe driving due to the phenomenon of sun glare. Although much evidence has been found to support that sun glare can highly impair one's visual performance, there are significant gaps in the knowledge and methodology dedicated to examining and quantifying the sole effects of sun glare on road safety.

The overall objective of this thesis is to gain a better understanding of the risks on the road network posed by sun glare and evaluate its safety effects in the city of Edmonton. To achieve this objective, a two-stage analysis was conducted. The first stage developed a methodology to model sun glare occurrence for the road network in the city, aiming to identify when and where a driver would be exposed to the risk of sun glare by considering different factors associated with the sun's position and road geographical conditions. Consequently, potential sun glare time windows were demarcated for each month over a typical year and corresponding glare prone locations were identified and plotted in a series of visualization maps, which can provide a reference to the public for identifying locations where sun glare is most prominent in city of Edmonton.

After identifying the glare prone locations, the safety risks at those locations during sun glare periods were assessed in the second stage. By contrasting the number of collisions during glare

and non-glare conditions, this second stage aimed to quantify the sole effects of sun glare on road collisions. A case-control design method was used to control for potential confounding factors related to weather condition, collision time/location, and travel direction. To test the significance of the differences in collision numbers, several statistical techniques were employed and included: chi-square test of independence, configural frequency analysis, and the Wilcoxon signed rank test. Ultimately, three major findings were concluded from the results of the collision analysis. First, sun glare was found to significantly contribute to collision occurrence, especially at road intersections. Quantitative assessments showed that collisions were expected to increase by about 30% under the condition of sun glare. Second, sun glare effects during mornings and evenings were observed to be especially worse in the months of spring and fall. Also, most of the daytimes in January, November and December, traffic safety in the southbound direction was significantly affected by sun glare. Lastly, certain collision maneuver types were over-presented during sun glare. It was found that the collisions due to signal violations and failing to yield to pedestrians and cyclist were over-presented at intersections. At mid-block locations, the proportions of collisions due to improper turning and lane changes were observed to be significantly higher.

Overall, the approaches proposed and developed in this thesis provide a new and innovative method to quantify the effects of sun glare on road safety. By linking sun glare exposure modeling with a thorough glare related collision assessment, this research helps to provide additional insights about the extent by which sun glare affects road safety. The findings from this thesis can be used to assist in alleviating the risks associated with sun glare in the planning and designing of future roads.

Acknowledgement

I would like to express my deepest gratitude to my supervisor, Dr. Karim El-Basyouny, who has inspired me by his devotion and dedication to research. His insights, guidance, patience, and support, greatly assisted me in completing my thesis. I am, therefore, fortunate to have him as my supervisor. I would also like to thank Dr. Tae J. Kwon, for his critical suggestions and continued support of my research. His insights helped me overcome several research challenges.

I would like to thank Dr. Liu for his time and willingness to participate in my final defense committee. I wish to thank Dr. Tony Qiu, Dr. Amy Kim, and all my course professors for guiding my research for the past two years and helping me to develop the necessary background in transportation engineering. Through their course work, I have developed a solid foundation in my thesis topic while gaining the appropriate experience and training in critical thinking, quantitative analysis, and academic writing.

I would like to thank Kexin Ren, Suliman Gargoum, Mostafa Tawfeek, Can Zhang and Naomi Li, for their help and advice over the past two years. Many thanks to all my other lab colleagues Maged Gouda, Karim Habib, Amr Mohamed, Jiangchen Li, and Kathy Tin.

Finally, special thanks to my family for their continuous encouragement, support, and love.

Table of Contents

List of Tables

List of Figures

List of Abbreviations

GIS	Geographic Information System
DEM	Digital Elevation Model
CFA	Configural Frequency Analysis
W test	Wilcoxon Signed-Rank Test

CHAPTER 1. INTRODUCTION

This chapter addresses current issues and challenges pertaining to the effects of sun glare on road safety. Section 1.1 provides background information on the topic of interest, and describes the factors affecting such phenomenon. In Section 1.2, the motivation of this thesis is described, followed by the objective and scope of the thesis stated in Section 1.3. Finally, the structure of this thesis is presented in Section 1.4.

1.1. Background

Clear vision is a basic component to safe driving on any road. The more visible the road environment is to a driver, the more likely it is for a driver to make safe and timely decisions when faced with road hazards. Any obstruction to a driver's vision could hinder their driving skills and thus reduce safety on roads. In fact, previous research has shown that decreased visibility significantly affects the traffic operation whereby increasing the risk of being involved in vehicular collisions (Ranney et al., 1999; Choi & Singh, 2005). Although roads are often designed in a way that meets minimum sight distance requirements, driver vision can still be obstructed by other environmental factors. Such factors include, but are not limited to poor lighting during nighttime and adverse weather conditions such as snow, fog, and rain (Wood & Owens, 2005; Andrey et al., 2001). All these factors are known to negatively affect drivers' visual perception (i.e., limited visibility and sight distances) and thus pose a huge threat to their safety (Andrey et al., 2001; Hermans et al., 2006). While many researches have considered assessing the risks associated with driving in poor weather conditions, only limited studies examined the road safety effects of sun glare, which is also found to be one of the significant causes of the vision obstruction (Auffray et al., 2008).

Figure 1.1 Sun glare in road traffic

Sun glare occurs when the sun is low in the sky horizon, usually an hour after dawn or before dusk. The direct sunlight exposure at a critical angle, which is normally less than 20° between the line of sight and the sunlight source, could result in temporary dazzling sensation to the observers, who may feel pain in their eyes (Churchill et al., 2012). An example of this phenomenon is shown in Figure 1.1. Such a temporary vision impairment, caused by sun glare, could result in negative impacts on the safety of all road users. Although sun visors are installed in most vehicles, little protection can be provided when the sun is close to the immediate horizon and when it occurs unexpectedly after making turns (Hagita & Mori, 2014). According to the National Highway Traffic Safety Administration (NHTSA), sun glare is reported as the main cause of a few hundred collisions that occur each year in the U.S (Staver, 2015). However, this figure is estimated to be under-reported as sun glare is rarely the sole cause of a collision and most drivers claim that they have been temporally blinded by the dazzle of sun glare. Another report from the Automobile Association in UK shows that there were 3,000 collisions related to sun glare blindness in 2013 (Massey, 2013). Glare times normally coincide with rush hours, making collisions even more likely to occur. Therefore, sun glare is one of the most significant safety concerns for the public and requires further research to reveal its nature and impacts on road safety.

1.2. Problem Statement

Evidence from previous research has shown that direct sunlight exposure is a significant casual factor that can cause vision obstruction and impair one's visual performance. Currently, however, there are significant gaps in the knowledge and methodology dedicated to examining and quantifying the sole effects of sun glare on road safety.

A study by Auffray et al. (2008) found that the presence of sun glare affected the distribution of traffic flow, leading to a drop in speed and a loss of homogeneity among the vehicles. The authors further claimed that it was difficult to quantify the sole effects of sun glare and future research was needed by further investigating direct impacts on road collisions. Several other studies in Japan and the U.S. investigated the relationship between collisions and the presence of sun glare, and found that sun glare contributed to collision occurrence (Choi & Singh, 2005; Hagita & Mori, 2014; Mitra, 2014). However, several persistent issues were found in most previous studies, such as not controlling for confounding factors, not considering the influence of the cloud cover, as well as the lack of identifying whether the collision locations are exposed to sun glare from a topographical perspective, and therefore they all require further examination.

Acknowledging the needs for new approaches to the problem of quantifying sun glare effects on road safety, this research is motivated to provide a better understanding of such effects and fill the gaps in previous research by combining the sun glare geographical analysis with a thorough collision analysis. Equally important, there were no previous studies that investigated sun glare effects in the city of Edmonton or across Canada. Nevertheless, the city of Edmonton, like most northern Canadian or European cities, is known to be one of the sunniest cities with more than 2,000 hours of bright sunlight each year according to the historical records from Environment Canada. This makes the city of Edmonton an ideal case study to investigate how sun glare affects traffic safety in the northern hemisphere.

1.3. Research Objectives

Sun glare, just like other environmental phenomena, could pose a significant danger to the safety of the travelling public. Despite the fact that only a few studies were conducted to analyze the effects of this phenomenon, the overall objective of this research is to evaluate the impacts of sun glare on road safety in the city of Edmonton, as a representative of most northern metropolitan cities. To achieve this objective, a two-stage analysis will be proposed.

In the first stage of the analysis, the aim is to develop a methodology to model the direct sun exposure for the road network in the city. Essentially, the method can be used to determine when and where the road is exposed to the risk of sun glare by considering different factors such as sun position and road orientations, thus making them vulnerable to road collisions due to the impaired visibility.

After identifying the glare prone locations, the safety risks at those locations will be assessed in the second stage. By contrasting the collisions between glare and non-glare conditions, this study aims to examine the direct impacts of sun glare on road safety from different aspects. In particular, three major research questions will be addressed in this research, which are:

1) whether sun glare has adverse effects on road safety in general;

2) whether sun glare effect is consistent among different months over a year; and

3) what types of collisions are over-presented under sun glare vision obstruction.

1.4. Structure of Thesis

This thesis consists of six chapters. The remaining thesis is organized as follows:

Chapter 2 provides a literature review on the impacts of sun glare related to road safety as well as the background knowledge of sun glare modeling.

Chapter 3 describes a list of data used in this research. The data collection work and research tools are also introduced in this chapter.

Chapter 4 presents an overview of the proposed methodology. In this thesis, a two-stage sun glare analysis method is introduced, which contains a sun glare occurrence analysis and a statistical historical collision examination.

Chapter 5 summarizes the results of the two-stage assessment and discusses the findings of the sun glare effects on road safety in the city of Edmonton.

Chapter 6 highlights the main contributions of this research and potential extensions for future work.

CHAPTER 2. LITERATURE REVIEW

This chapter provides a review of previous studies related to sun glare. Section 2.1 summarizes the investigations of sun glare effects on road safety. Section 2.2 describes the background knowledge of sun glare modeling as well as its contributing factors. The summary of this chapter is presented in Section 2.3 with the discussion of limitations of pervious research.

2.1. The Impacts of Sun Glare on Road Safety

Several previous studies have considered assessing the risks associated with driving in poor weather conditions, such as rain, snow and fog, but only limited research examined the effects of sun glare on road safety. However, there is enough evidence supporting the fact that direct exposure to light can cause strong discomfort to the eyes and impair the visual performance. According to Schreuder (1968), sun glare generally happens when the rays of sunlight fall directly into the line of sight, which can "wash out" an image on the retina and cause temporary blindness.

In addition, Auffray et al. (2008) pointed out that there are usually three components of sun glare effects: vision disability, discomfort sensation, and recovery time. The disability effect is a kind of visibility impairment caused by light scattering in the eye and it is in this period that speed reduction, collisions, and car pile-ups have a higher probability to occur. Some studies investigated the glare effects of light from headlamps and it is commonly considered that headlamps and direct sunlight affect visibility in a similar way (McGwin et al., 2000; Theeuwes et al., 2002; Babizhayev, 2003; Auffray et al., 2008). According to the findings from these studies, the reflections off the dashboard and windshield can also cause a situation known as vailing glare in addition to the dazzling caused by the direct exposure to glare. Although the drivers can see through the "veil", the front view is not captured clearly and this threatens driving safety. The studies also indicated that people do not perform in the glare in the same way and their reactions depend on age, visual health, and intensity of glare.

Among the limited number of studies examining sun glare effects on road safety, some examined impacts on driving behaviors, while others investigated the direct relationship between collisions and the presence of sun glare. Concerning driving behaviors, Ayres et al. (2004) conducted a study of speed adjustment to sun glare through video observations on two public roads in both glare and non-glare conditions. A decrease in speed and an increase in speed variability were found on vehicles approaching a setting afternoon sun. These effects were similar to what had been reported in fog and other visibility-impaired conditions and were found to have a strong association with an increase in collision risk (Shepard, 1996).

Another study carried out by Daniel and Chien (2009) analyzed traffic speed during adverse weather conditions and found that the vehicle speeds at potential sun glare time periods were lower than other times. A study by Auffray et al. (2008) conducted a regression analysis using data collected on an American freeway to examine the potential relationships between measured traffic characteristics and sun glare. The investigation indicated that the presence of sun glare affected the distribution of speed and flow, as well as created bottlenecks at specific locations. The authors believed that the restriction of capacity could lead to a decrease in speed and a loss of homogeneity in traffic flow, which would pose a risk to traffic safety. However, the study also pointed out that it was difficult to quantify the sun glare effects strictly and future research was needed by investigating different locations and patterns, as well as direct impacts on road collisions (Shepard, 1996).

In terms of safety assessment, a study conducted by Choi and Singh (2005) used descriptive statistical and contingency analyses to explore the association between reported collisions and sun glare. The authors found that sun glare was a contributing factor to collisions and people over 55 years old were more likely to get involved in collisions if affected by sun glare. Moreover, the study also showed that roadway geometry and number of lanes also played an important role in collision occurrence related to sun glare. In Japan, Hagita and Mori (2014) carried out an analysis using 5 years of collision data and computed the sun position relative to each collision to identify the presence of sun glare. The results showed that the collision rate was higher when the sun was in front of the vehicle, especially for pedestrians, bicycles and

intersection collisions. In another study in Tucson, Arizona, an empirical investigation was conducted by Mitra (2014) to assess the sun glare effects on intersection safety. The author used 4 years of collision data on signalized intersections and compared those exposed to sun glare with those unaffected by the glare. The analysis showed that sun glare contributed to the intersection collision occurrence and the adverse effect was greater in early spring and fall months. It was also found that right-angle and rear-end collision rates were higher during the glare periods.

Although the previous literature showed some insights of adverse impacts of sun glare on road safety, two major limitations were found in most previous studies. First, many confounding factors were not precisely controlled for when conducting the comparison between glare and non-glare conditions. In particular, studies did not examine collisions at the same location or time of day and did not address the influence of cloud cover. Since all these factors are highly associated with the collision exposure in terms of different aspects such as traffic volumes and road geometry features, it is important to control for these elements when assessing the safety effects between the presence and the absence of sun glare.

Second, previous studies were only conducted along one particular arterial or some arbitrary locations, without identifying whether the collision locations were exposed to sun glare from a topographical perspective. Since the sun position changes throughout the year, locations that are potentially impacted by sun glare will not be consistent. Therefore, the glare prone locations may vary and need to be identified specifically over different months of the year; otherwise it remains unclear whether the locations analyzed in previous studies were under the risk of sun glare or not. Without identifying such topographical characteristics, some collisions may have been mistakenly considered to be caused due to glare, leading to an over- or under-estimation of sun glare safety effects in the previous assessment.

A possible approach to overcome such deficiencies and limitations presented in previous studies will be to develop a method to characterize the road network of the entire city with sunlight exposure, and to investigate when and where sun glare is a safety risk to the road users.

2.2. Sun Glare Modeling

To explore the effect of sun glare on road safety, it is important to know how sun glare is captured, and when and where the road is exposed to the risk of glare. According to previous literature, there are four main factors that determine the occurrence of sun glare, which are the position of the sun, the angle of glare, the configuration of the terrain and the weather condition (Jurado-Pina & Pardillo-Mayora, 2010; Auffray et al., 2008). The following sections describe each factor in detail.

2.2.1. Sun Position

The position of the sun at a given time and location is usually defined in local coordinates by the azimuth angle and the elevation angle. The azimuth angle is the sun's relative positions along the horizon, and measured clockwise from north ranging from 0° to 360°. The elevation is the angle measured up from the horizon, with 0° at the horizon and 90° directly overhead of the terrain (Auffray et al., 2008). The solar geometry is shown in Figure 2.1. There are a number of astronomical algorithms, which can be used to calculate these local coordinates for the sun position, some of these include the algorithm by Walraven (1978), the algorithm by Michalsky (1988), and the algorithm by Grena (2008). Since the focus of this thesis is not on how the sun position is calculated, this issue will not be described in any more detail. In this research, the sun position is obtained from the Sun Earth Tools website (www.sunearthtools.com), which applies Michalsky's algorithm to calculate the sun positions relative to specific locations. In order to focus only on the collisions that are affected by sun glare, the Michalsky's algorithm is also applied manually to calculate the solar position for each selected collision during the glare time window according to its time and location. The detailed steps related to the extract of glare related collisions are described in Section 4.2.1.
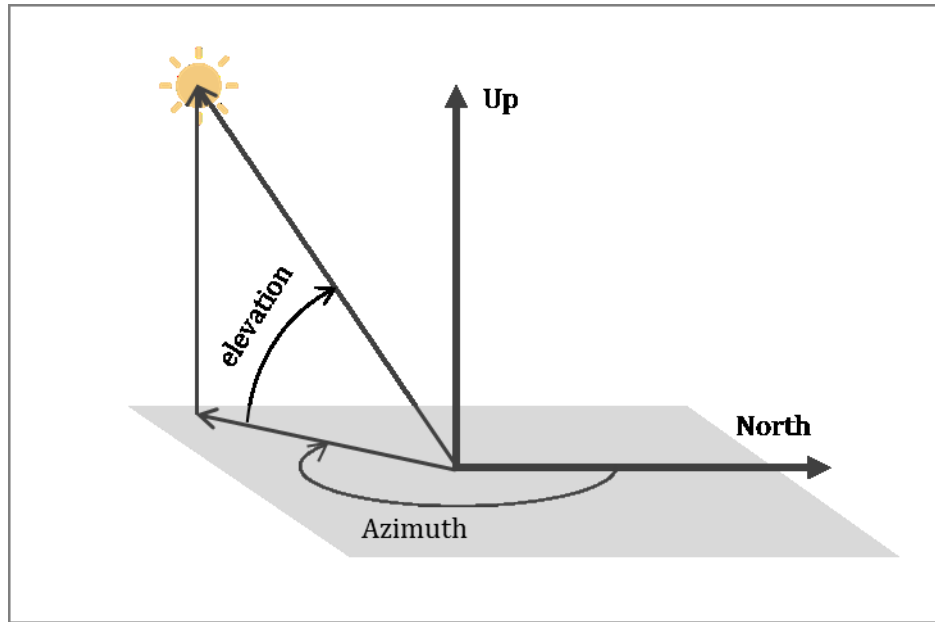
Figure 2.1 Solar position coordinates

2.2.2. Sun Angle

It is widely recognised that sun light interferes with a driver's visibility when the sun is low in the sky and the light falls directly into their eyes, causing a short-term blindness (Auffray et al., 2008). Many studies have shown that the disability caused by the sunlight highly depends on the angle between the line-of-sight and the glare source. Based on a mathematical equation for the veil luminance, Jurado-Pina and Pardillo-Mayora (2010) determined the disability glare cone angle to be 19° and 25° for drivers aged 40 and 60 years, respectively. They also indicated that the line of sight was directed to a point 90 m ahead of the driver's position on the road's centreline, and that the road azimuth direction was assumed to be consistent with the driver's line of sight. Another study by Churchill et al. (2012) indicated that sun glare occurred when the centre of the sun lied in the areas swept out in both the horizontal and vertical planes. As a result, the authors suggested a 20° maximum angle for the both the horizontal and vertical ranges. Similarly, Auffray et al, (2008) also determined the presence of sun glare by looking at the elevation angle and azimuth angle individually. However, they argued that there was no definite reference for identifying sun angles for glare to vehicles, and intuitively chose 0°-15° as the

angle range to demarcate possible glare time intervals. In another study by Hagita and Mori (2013), the solar position was calculated at the time and location of each collision. After assessing the collision rate, they concluded that when the sun was low in the sky with the elevation angle between 10°- 40°, and that the driver vision was adversely interfered by the sun glare. Although these previous findings were mixed, it can be found that a sun angle of 20° was acknowledged to cause glare in most of these studies. This is also consistent with the finding from Zwahlen (1989), which suggested the maximum angular distance for one's visibility to be normally 20°. Therefore, the angle limit of 20° is chosen for the sun glare issue from both horizontal and vertical geometrical perspective in this research.

2.2.3. Terrain Configuration

Depending on the surrounding terrain configuration, the sun beams may be blocked from driver's line-of-sight at certain angles. For this reason, Jurado-Pina and Pardillo-Mayora (2010) defined a terrain profile by pairing azimuth and elevation values, which covered the visual field at a specific location to identify the sun glare coverage. A recent study by Khumalo (2014) demonstrated a large-scale implementation of digital elevation models (DEM) to efficiently generate shadow areas by considering a specific time and location of interest using a tool available in ArcGIS (Khumalo, 2014). However, Mitra (2014) also pointed out that on a flat terrain, which is the case for this study, the relative position of the sun to driver's eyes and the direction of travel are the most important factors that should be considered when identifying sun glare.

2.2.4. Weather

Since weather factors such as precipitation and fog can highly affect the occurrence of collisions, many studies have pointed out that it is important to segregate the effect of sun glare when analyzing its impacts (Hagita & Mori, 2014). However, it is difficult to calculate glare permitted conditions at daytime using the existing weather data because the precise weather information at a specific collision time and location is very limited (Mitra, 2014). Furthermore, inherent limitations and challenges associated with lack of cloud cover information, it becomes almost

impossible to evaluate the percentage of sun glare during cloudy days (Auffray et al., 2008). Alternatively, according to Auffray et al. (2008), the analysis can be focused on only two extreme sky cover conditions: clear sky with presence of glare (i.e., glare case) and overcast sky with the absence of glare (i.e., control case)

2.3. Summary

Chapter 2 presented a review of literature on two topics: impacts of sun glare on road safety and sun glare modeling. It is found that there is sufficient evidence to support the fact of visual impairment caused by sun glare, but limited research has been done to understand how sun glare would affect road safety. Although these few studies showed some insights of adverse impact of sun glare on road safety, several issues such as not controlling confounding factors, not considering the weather conditions, as well as the lack of identifying whether the collision locations are exposed to sun glare from a topographical perspective, were still found and required further examination. As for sun glare modeling, four major research issues were identified based on previous studies, which are position of the sun, the angle of glare, the configuration of the terrain, and the weather condition. All four factors need to be properly addressed when identifying the occurrence of sun glare.

To address the gaps in previous studies, a two-stage safety assessment is proposed in this thesis. First, sun exposure is modeled for the entire city of Edmonton to identify areas where sun glare is prominent as well as the corresponding glare time window. After identifying the glare prone locations, the safety risk at those locations will be assessed based on 5 years of collision data which was matched with the corresponding weather data. By carrying out a case-controlled comparison, this study aims to provide a better understanding of the sun glare effects on road safety while providing insight to help alleviate the risk in the future planning and designing of roads.

CHAPTER 3. DATA

This chapter presents a detailed description of the data used in the thesis. A total of four datasets including GIS data, sun position data, historical collision data, and hourly weather data, were obtained and analyzed. Since large amounts of datasets are to be assimilated, a geographical information system (GIS) based platform was used to effectively manage the data in this study. GIS has long been recognized as a powerful yet efficient tool, particularly for spatial data management since it can bring about more rapid handling and processing of any data with locational attributes. For this reason, GIS is widely adopted by transportation and climate research communities as a main platform to better facilitate model accessibility, database maintenance and updating, and cartographic display of model results. All data sets collected in this study were spatially analyzed using various tools available in Esri's ArcGIS, which is the industry standard in GIS software (ESRI, 2016). Specifically, the version 10.4 of ArcGIS Desktop was used.

3.1. GIS Data

This research aims to explore the effects of sun glare on the road network in the city of Edmonton, which is the northernmost city of North America with a population over one million. It is located at 53° 32' 45.1788'' N latitude and 113° 29' 24.4032'' W longitude with a time zone of UTC-7:00. The coordinate information was used as the base input when calculating positions of the sun. Since Edmonton is located at a high latitude, the daytime varies significantly among different seasons, which last more than 17 hours in summer, while only 8 hours in winter. This makes the city of Edmonton an ideal case study to investigate how sun glare affects traffic safety in the northern hemisphere. Nevertheless, it is worthwhile noting that the conclusions about sun glare effects in Edmonton may not be directly applicable to other cities

A shape file containing Edmonton's road network was obtained from the Office of Traffic Safety, City of Edmonton, and used as the base map in this research. A shape file is a geospatial vector data format for GIS software, which stores the location, shape, and attributes of geographic

features ("Shapefiles: ArcGIS online help," n.d.). The road network is a typical east–west/north–south grid type and is shown in Figure 3.1. According to the spatial features and satellite images, the downtown area, where the tall buildings are mainly located, was also identified on the map which was used as the reference for excluding the roads in shades. In addition, a digital elevation model (DEM) for the city of Edmonton was also obtained through the open data source provided by AltaLIS (www.altalis.com/). The DEM refers to a digital model of terrain's surface from its elevation data (Khumalo, 2014). In this research, the DEM was derived from a series of mass points and breaklines with corresponding elevation values at a resolution of 10 meters. Figure 3.2 shows the resulting DEM raster, which indicates the elevation of Edmonton ranging from 594 to 771 meters high. As can be seen from this figure, most of Edmonton's terrain is quite flat and the areas with significant topographical changes are mainly located along the river valley. For more information about how to create DEM, readers may refer to the online resources provided by ESRI (http://support.esri.com/).
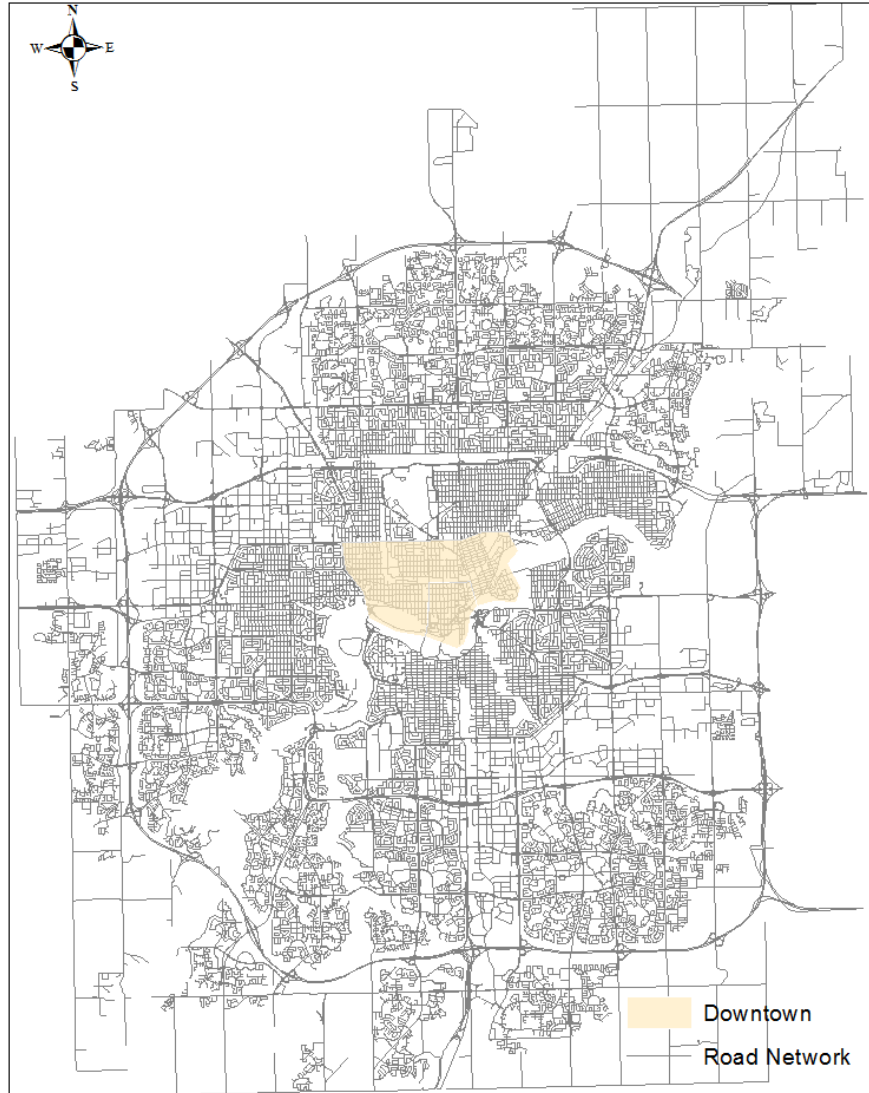
Figure 3.1 Road network GIS map of city of Edmonton

Figure 3.2 Digital elevation model of city of Edmonton

3.2. Sun Position Data

As previously described, the azimuth and elevation angles are the two most important local coordinates that define the position of the sun. In this research, these two local coordinates for the city of Edmonton were extracted at an interval of 5 minutes throughout a typical year using an online tool available at SunEarthTools website (www.sunearthtools.com.) This tool

implements Michalsky's algorithm to precisely calculate the sun positions for a specific location. It is normally assumed that there are no significant differences between the sun's position at the same exact time and date, for each location, from one year to the next (Auffray et al., 2008; Mitra, 2014). This assumption was also confirmed by analyzing the sun position data from the above-mentioned website. Therefore, the sun position data for this study was extracted based on the calculation for each day in the year of 2009. As the discussion based on previous studies in Section 2.2.2, critical angle limit of 20° was chosen for identifying the sun glare time windows based on the sun elevation. Once the glare time windows are set up, the corresponding solar azimuth ranges for each month can be extracted and used to further identify the glare prone locations. A detailed description of the sun glare occurrence analysis is presented in Chapter 4.

3.3. Collision Data

To investigate the sun glare effects on road safety, 5 years of traffic collision data spanning from 2007 to 2011 for the city of Edmonton was used. The collision database is maintained by the City of Edmonton based on police reports. It includes detailed information for each collision such as time, location, collision types and corresponding travel directions of at-fault vehicles. Since the exact longitude and latitude for each collision is known, all collisions were plotted in ArcGIS and overlaid with the road network layer for further analysis. In this study, only collisions occurred during weekdays were selected for the analysis to exclude any differences in traffic flow behavior.

3.4. Weather Data

To identify the occurrence of sun glare, it is necessary to acquire detailed weather information as it will later be used in conjunction with the collision data such that the weather condition can be estimated for each specific collision. In this research, the weather data for Edmonton was obtained from the weather reports collected at Edmonton International Airport weather station from Environment Canada (Environment Canada, 2013). Hourly weather data was extracted for each day from 2007 to 2011 to match the available time range of the collision data. The extracted weather data includes temperature, wind speed, precipitation, visibility, and sky coverage

condition. The airport weather station is located at 25km south to the center of city of Edmonton so that its reported weather conditions may not precisely represent the conditions across the entire city. However, this study focuses on only two extreme weather conditions: clear weather and overcast weather, under which it is expected that there would not be significant weather variations across the city. As such, the weather data from this station was assumed to be representative for the whole city in this study. Besides, the weather data collected at the International Airport station was found to be the only available data source that contains detailed historical weather records including cloud cover condition. Due to the limit of obtaining more advance data with specific weather information for different road segments or from an even closer station, the weather data from Edmonton International Airport is considered the most ideal choice for conducting this study.

CHAPTER 4. METHODOLOGY

Recognizing the complexity of quantifying the sole impacts of sun glare on road safety, a unique two-stage safety assessment method is proposed and described in this chapter. The first stage is to conduct a sun glare occurrence analysis in an attempt to model the sun light exposure for Edmonton's entire road network. This can be achieved by first determining the potential sun glare time windows observed over different months of the year as well as its corresponding glare prone locations, as described in Section 4.1. Section 4.2 details the second stage, where the goal is to conduct a collision analysis based on the identified locations by assembling suitable comparison data and carrying out statistical analyses. Three statistical techniques including the Chi-square test of independence, configural frequency analysis, and the Wilcoxon signed-rank test, are also introduced in this section that are used to investigate sun glare effects on collisions. A flowchart summarizing these processes is shown in Figure 4.1
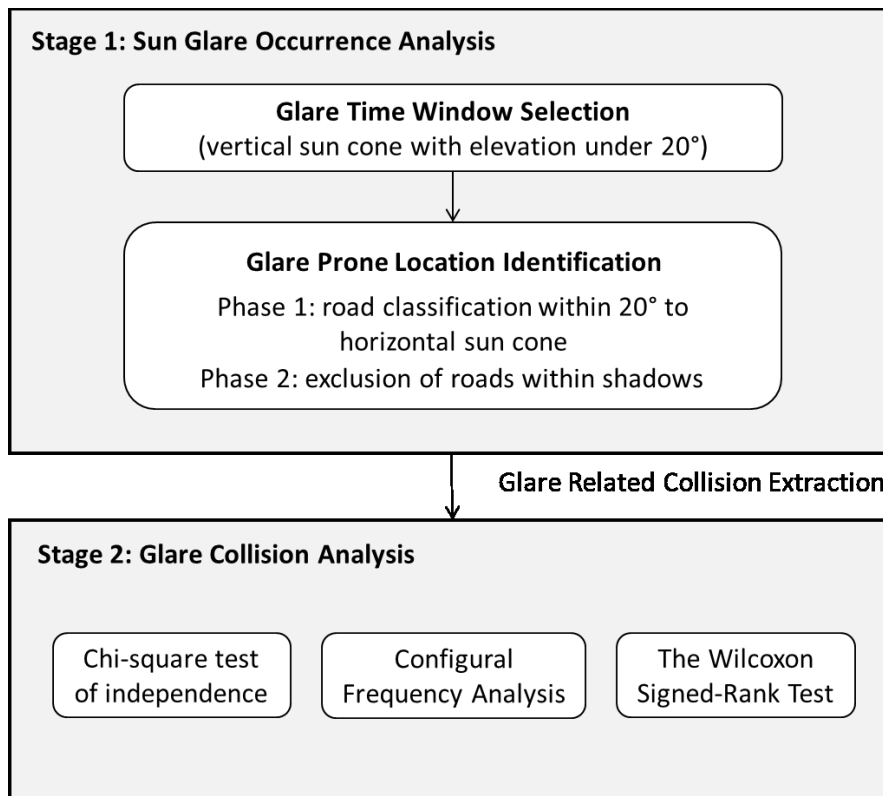
Figure 4.1 Methodological approaches flow chart

4.1. Potential Sun Glare Prone Time and Areas Identification

The literature identified four main factors to determine the occurrence of sun glare, which are the position of the sun, the angle of glare, the configuration of the terrain, and the weather condition. To address the two most important factors which are the position of the sun and the angle of glare (Mitra, 2014), it is commonly required for the vertical and horizontal roadway geometries to point directly into the sun (Auffray et al., 2008). The geometrical conditions can be illustrated as shown in Figure 4.2. Thus, in this stage, a potential glare time window was first identified for modeling the vertical angle of glare based on the extracted sun elevation data. With the identified glare time windows, the corresponding sun glare risk locations were then identified by considering the horizontal geometry. Since Edmonton's terrain is quite flat and the safety assessment is based on a citywide analysis, it is expected that the terrain configuration will not affect the final results in any meaningful way. However, a Hillshade map was introduced in this study to propose a way to account for shadow effects. Lastly, the influence of weather factors is discussed in the collision analysis.
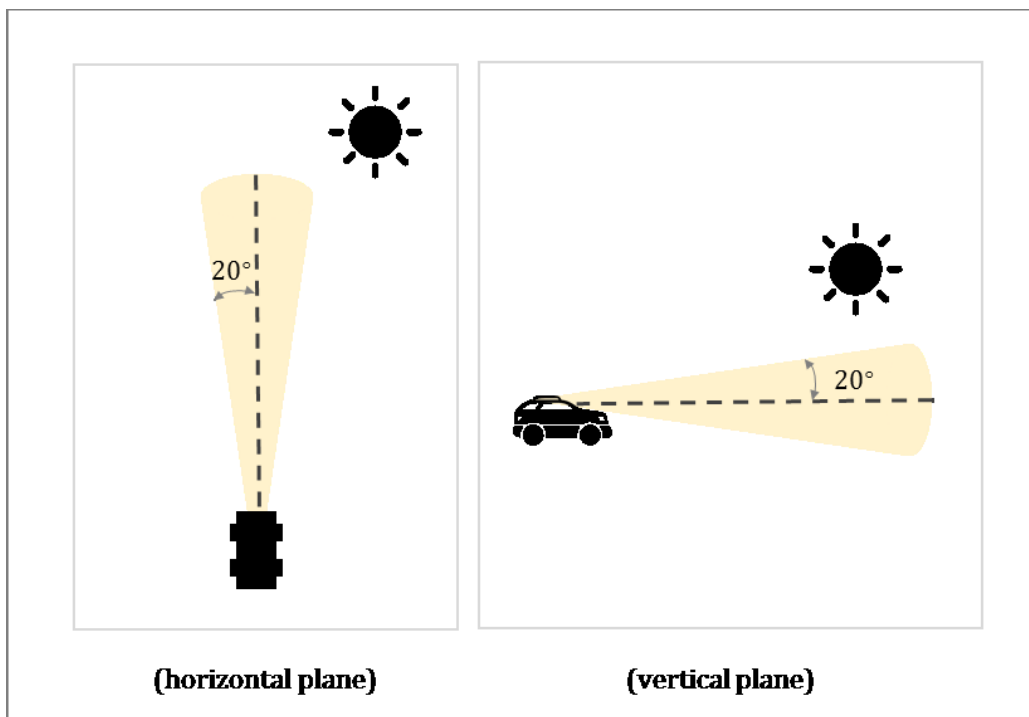
Figure 4.2 Geometrical conditions of sun glare

4.1.1. Glare Time Window Selection

Since sun glare usually occurs when the sun is low in the sky, two glare time windows, morning glare and evening glare, were identified. Also considering the position of the sun, which is inconsistent among different months, varying rather than fixed time windows were computed based on the sun elevation for each month over a typical calendar year. In this study, sun elevation angles between 0° and 20° were chosen as a reasonable range based on previous literature to demarcate a potential glare occurrence. The glare time window of each month was calculated by finding the intersection of the time intervals with low sun elevation of each day in the month. This method ensures that the identified glare time window can represent a consistent condition for the sun for the whole month. This means that during the identified time window, the sun always has a glare risk elevation in each of the month. These time windows are shown in Table 4.1.

Table 4.1 Typical Sun Glare Time Windows for Edmonton

	Morning Glare		Evening Glare	
Months	**Time Windows**	**Sun Azimuths**	**Time Windows**	**Sun Azimuths**
February	8:20-10:00	112.3°-139.5°	15:30-17:15	223.8°-241.7°
March$_{1-7th}$	7:20-9:45	99.0°-132.1°	15:45-18:15	228.9°-259.1°
March$_{15-31th}$	7:45-9:30	88.6°-113.1°	17:45-19:40	249.6°-268.3°
April	7:05-8:30	74.7°-97.7°	18:45-20:10	270.2°-279.6°
May	6:00-7:45	58.8°-83.5°	19:15-21:05	280.4°-297.9°
June	5:10-7:45	48.5°-78.8°	19:30-21:50	283.3°-309.0°
July	5:50-8:00	54.28°-83.0°	19:30-21:30	282.6°-302.3°
August	6:45-8:15	68.42°-93.4°	19:00-20:20	272.9°-284.3°
September	7:30-9:00	84.4°-111.5°	18:00-19:10	255.4°-264.9°
October	8:30-10:00	105.19°-131.6°	16:30-18:00	230.9°-246.3°
	Winter All Daytime Glare			
Months	**Time Windows**	**Sun Azimuths**		
January	8:50-16:25	129.5°-230.5°		
November$_{8-30th}$	8:30-16:20	127.4°-232.5°		
December	9:00-16:00	132.7°-226.1°		

It was found that during three months in winter, November, December and January, the sun was always low in the sky with an elevation under 20° during all daytime. Thus, instead of identifying specific morning or evening glare time windows for those 3 months, all the daytime was considered to have the potential of sun glare risk and analyzed separately as a special case in

Chapter 5. To simplify the analysis, the effects of daylight saving time change on the position of the sun, in March and November, were eliminated by excluding the days of March 8-14 and November 1-7 since the respective time change occurs on Sundays in those ranges each year. Once the glare time windows were set up, the corresponding solar azimuth ranges (sun cone) for each month were extracted using a similar algorithm to find the intersecting parts of each day. The identified solar azimuth is also shown in Table 4.1 and is used to further identify the glare pone locations in the next step.

4.1.2. Sun Glare Prone Location Identification

With the previously defined sun glare time windows for both morning and evening period in different months, the corresponding locations were identified based on the GIS road network and DEM of the city of Edmonton by using ArcGIS. There are two main phases included in this section: road orientation classification according to azimuth sun cone, and exclusion of shaded areas as described in Sections 4.1.2.1 and 4.1.2.2, respectively (Khumalo, 2014).

4.1.2.1.   Road Orientation Classification According to Azimuth Sun Cone

This phase was carried out to address the angle of glare from a horizontal geometrical perspective by matching the road network alignment with the sun position. To achieve this, three steps were carried out in ArcGIS including changing road segments from polylines to single lines; calculating the road bearings; and carrying out a road searching within the 20° to the sun cone. These steps are discussed as follows, in the respective order.

- **Road network segmentation:** To make the road network data manageable, the road network (polylines) was first divided into straight line segments with constant direction, which is the basis for the methodology of this phase and allows for the following establishment of road bearings. This step was achieved by the Split Line at Vertices tool in ArcGIS, which splits the road network polylines at each vertex and creates multiple line features so that each segment has a unique bearing. An illustration of the input and output of the Split Line at Vertices tool is shown in Figure 4.3. After splitting the road

22

network, each segment was assigned to a unique identifier, based on which a road bearing is calculated in the next step.
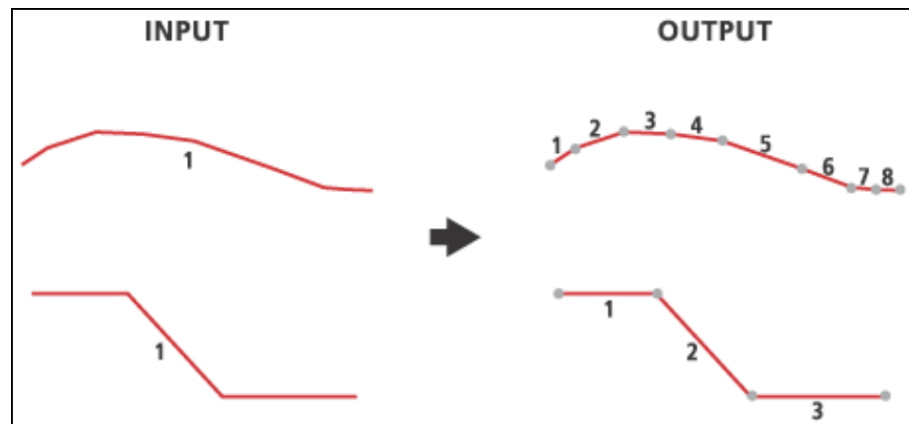
Figure 4.3 Split lines at vertices (ERSI, n.d.)

- **Road bearings calculation:** With the split road segments, the Linear Directional Mean tool in ArcGIS was employed to calculate the bearings, which is the mean direction for each line segment calculated from the North, ranging from 0° to 180°. Reverse bearings were also calculated by adding 180° to these bearings. Once the bearing for each road segment is known, an attribute query can be done to extract the locations with the risk of sun glare.

- **Selection of roads within 20° to the azimuth sun cone:** With the identified sun azimuth range during the designated time window in each month, an attribute query was performed to select the roads, whose alignments matched the sun azimuth. This step was done using the selection tool in ArcGIS and the road segments with bearings or reverse bearings within a 20° angle difference to the sun cone were selected (Churchill et al., 2012; Jurado-Pina and Pardillo-Mayora, 2010). The outcome of the query is the locations, which are considered to have the potential risk of sun glare with their corresponding time window in each particular month. Identified locations in this step were used to extract the related collisions in the following analysis phase. However, a sun position algorithm was applied manually to further check the occurrence of sun glare at each collision time

snapshot in order to exclude any non-sun glare related collisions. The vehicles with different travel directions on the same locations are discussed and analyzed in the collision analysis section.

4.1.2.2.   Exclusion of Shaded Areas

The objective of this phase is to address the factor of terrain configuration and exclude road segments in shadow areas. A Hillshade tool of ArcGIS was employed to model the sun light illumination of a surface to identify the shade areas on a DEM raster. Once the sun coordinates are input, the Hillshade tool sets a position of the light source and calculates the illumination value for each cell in the raster in relation to neighboring cells. The output of such is a shaded relief raster that considers both local illumination source angles and shadows, and indicates the illumination value of each cell ranging from 0 to 255, with 0 representing complete shade and 255 the brightest. Afterwards, a Reclassification tool was used based on the hill shade output layers to pick out the pixels in complete shade so that shadow maps were created. The shadow maps were then converted from raster to polygon and erased from the classified sun glare prone locations determined in the previous phase. Ultimately, only the road segments with direct sun exposure were left and the roads within shadows were excluded from further analysis. The process of making shadow maps is illustrated in Figure 4.4, which takes the morning glare period in September as an example. The map in the left side of the figure shows the output layer of Hillshade raster and the map in the right side is the shadow map, which sorts out the pixels that are in complete shades.
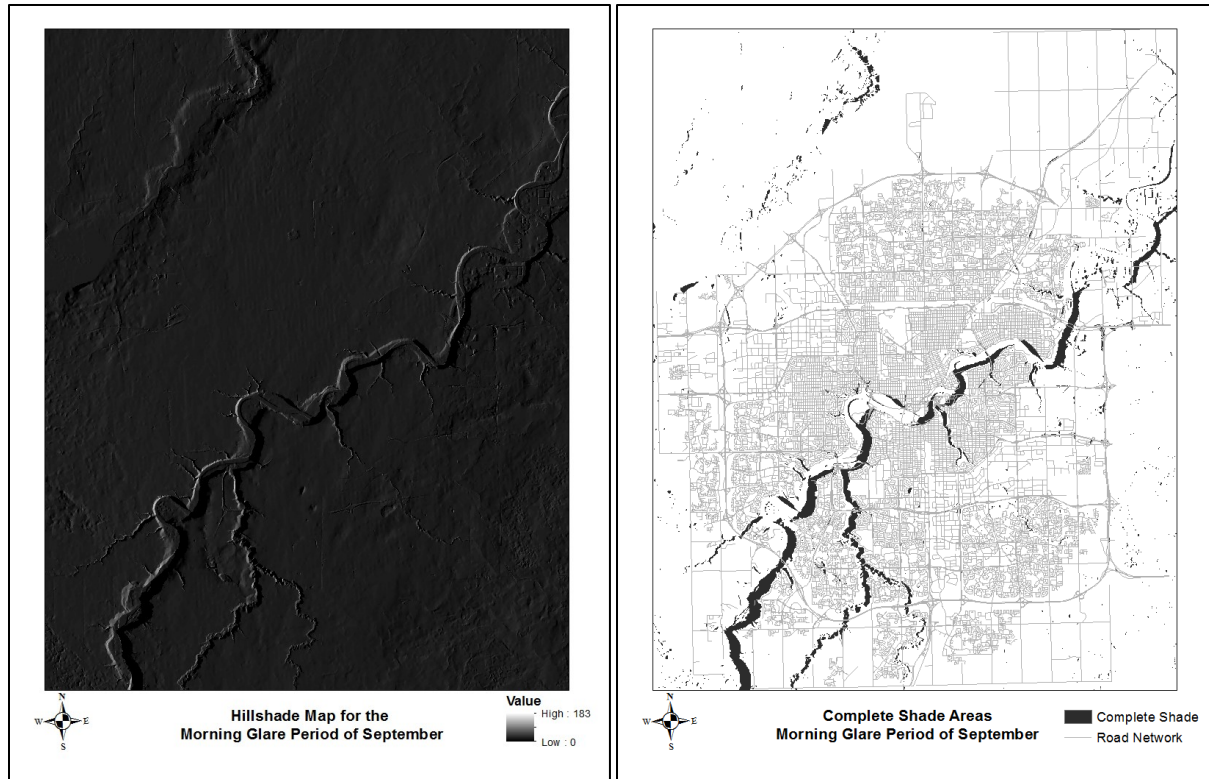
Figure 4.4 Production of the Shadow Maps

For each glare time period identified in each month, two shadow maps were created considering two extreme conditions, which used the lower and upper values of the corresponding sun glare azimuth range, respectively, and a low elevation of 5° for the input of the sun coordinates. The two shadow maps were then merged into one layer for erasing the roads in complete shade. As for the shadow presented behind buildings, the downtown areas, where tall buildings are mainly distributed in Edmonton were also erased from the glare prone road selections. As can be seen on the DEM and shadow maps, most of the shade areas are located along the river valley, which hardly overlaps with the City's road network. Thus, it can be expected that the final output map layers of this step can represent the sun glare prone locations for the road network of Edmonton in a meaningful way. It should be noted that the methodology described herein proposes a way for future research to account for the terrain influences. If a more detailed DEM is available, the methods can be applied to calculate the exact sun exposure of a particular location for each time snapshot.

4.2. Statistical Techniques for Collision Analysis

4.2.1. Collision Data Extraction and Assembling

In order to directly investigate sun glare effects on road safety, historical collision data with the potential of sun glare involvement was extracted and assembled for examination. For each month, collisions that fell in the glare time windows as well as those that occurred at the identified locations were selected and extracted. A case-control design method was used to control for potential confounding factors related to weather condition, collision time/location, and travel direction.

In this study, the potential sun glare occurrence was considered as an exposure. To exclude the effects of other adverse weathers, only two weather conditions were examined, which corresponded to clear and overcast weather. The case group and control group were developed based on the observed collisions under the two weather conditions, respectively. As vehicles with different travel directions on the same road have different sunlight exposure, the collisions in each group were split according to the travel direction of the vehicle at fault. By examining the sun position data for Edmonton (as seen from Table 4.1), it is intuitive to assume that eastbound traffic would be exposed to sun glare in the morning glare period and westbound traffic would be exposed in the evening glare period. Therefore, the travel direction for each collision was used to indicate if exposure to sun glare was evident or not. Finally, collisions in each condition indicated above were summed for each month and aggregated for the analysis of overall effects. The layout of the final data is shown in Table 4.2. Except for the case with sun glare exposure controlled by the cloud cover, the control group are found to be comparable to the case group in terms of time of day and location. Therefore, it can be expected that the difference of collision frequencies among different directions are caused by the exposure to the sun glare.

The collision analysis was divided into two parts according to the locations: intersection-based and mid-block collisions. The summary of intersection collisions counts and mid-block collisions are shown in Table 4.2 and 4.3, respectively. It should be noted that there were only two directions (east and west) counted for mid-block crashes in the morning glare and evening glare

periods, as only the roads with east-west orientation matched with the sun azimuth were involved in the collision extraction. Besides, to further check the sun position for each collision and exclude the unrelated collisions, the Michalsky's sun position algorithm was applied on each collision to calculate the specific sun position based on its collision time and location. As each collision was geocoded with the road segment, the calculated sun position azimuth was compared with the bearings of the road segment where the collision occurred. For intersection collisions, the bearings of all approaches related to the intersection were considered and compared with the sun. As a result, the collisions with a road or approach bearing differing above 20° with the sun azimuth were removed from the analysis, and only the collisions that occurred on a location with a potential sun glare risk were included in the statistical analysis. The detailed steps of the sun position algorithm can be found in Michalsky (1988).

Table 4.2 Observed Intersection Collisions over Different Glare Periods and Directions

Glare periods	Months	Group*	Travel Directions			
			East	West	North	South
Morning Glare	Feb-Oct	Case	258	224	184	208
		Control	250	245	290	264
Evening Glare	Feb-Oct	Case	262	241	251	205
		Control	294	227	328	257
Winter All Daytime Glare	Nov, Dec, Jan	Case	360	343	348	400
		Control	499	483	530	486

*Group includes "Cases" which refers to collisions under the clear weather condition and "controls" which refers to collisions under overcast weather condition.

Table 4.3 Observed Mid-block Collisions over Different Glare Periods and Directions

Glare periods	Months	Group*	Travel Directions			
			East	West	North	South
Morning Glare	Feb-Oct	Case	227	181	-	-
		Control	200	222	-	-
Evening Glare	Feb-Oct	Case	132	144	-	-
		Control	152	182	-	-
Winter All Daytime Glare	Nov, Dec, Jan	Case	5	4	194	132
		Control	8	10	274	180

4.2.2. Chi-Square Test of Independence

A chi-square test of independence was used in this study to determine whether there is a significant statistical relationship between sun glare and collision occurrence in each glare time period. This technique is usually applied to detect the association between two categorical variables in a contingency table, which fits our assembled data in section 4.2.1. The two categorical variables were set as the weather conditions (case or control) and collision directions, and the collisions numbers in each cell were used as the observations. As previously described, the clear weather indicates the occurrence of sun glare on the identified locations while the overcast weather does not, and the collision direction indicates whether the driver's line of sight is aiming towards the sun or not. It is considered that sun glare occurs when the collision direction is directly towards the sun in a clear weather condition. Thus, the relationship between these two variables could reflect the association between sun glare and collision frequency. In this study, the null hypothesis was set as the two variables were independent, indicating that the sun glare was independent of the collision occurrence. In contrast, the alternative hypothesis was established to state that the sun glare would affect the collision occurrence, with an expected higher number of eastbound collisions in the morning and higher number of westbound collisions in the evening.

To conduct the chi-square test, the first step was to calculate the expected frequencies E of each cell in the contingency table under the null hypothesis of independence. Then, the chi-square

statistic was calculated to compare the difference between the observed and expected counts. The equations are shown as below.

$$E_{i,j} = N * p_{i.} * p_{.j}$$
(4-1)

$$p_{i.} = O_i/N; \quad p_{.j} = O_j/N$$
(4-2)

$$\chi^2 = \sum_{i=1}^{r} \sum_{j=1}^{c} \frac{(O_{ij} - E_{ij})^2}{E_{ij}}$$
(4-3)

where, χ^2 denotes the chi-square test statistic; O_{ij} denotes the observed frequencies; E_{ij} denotes the expected frequencies; N denotes total numbers of observations; r and c indicate the number of rows and columns in the contingency respectively. The chi-square statistic asymptotically approaches a chi-square distribution and can be then used to calculate a p-value based on the chi-square distribution. The degree of freedoms is equal to $(r-1) * (c-1)$.

4.2.3. Configural Frequency Analysis

The Configural Frequency Analysis (CFA) is a widely used statistical method for multivariate data analysis, which has the advantage of being non-parametric and not requiring extensive computation. The goal of this method is to detect types and antitypes in cross classification of categorical variables, which is also the case in the assembled data in this study. Types are defined as patterns of variable categories that occurred significantly more than expected by chance, while antitypes are those patterns that occurred significantly less, both of which are identified by comparing observed and expected frequencies in individual cells (configuration patterns). Instead of just determining correlation between variables, the focus of CFA is to examine whether certain patterns stand out in case of significantly more or less than expected based on a priori specified assumption. From these detected patterns, the researchers can interpret whether certain variable values in different categories generally occur together and are statistically related from a person-oriented perspective. In this study, the CFA was employed to determine whether there were significant collision differences between glare and non-glare

weather conditions, and thus to interpret the sun glare effects on collision risks and driving behaviors. To perform a CFA, three main routine steps were conducted as below:

- First, a CFA base model (i.e., chance model) needs to be selected to calculate the expected frequencies. As described in most publications, the classical and most common base model is the *First Order CFA model*, which assumes that no variable relationships exist, except the main variable effects. The base model can be contradicted if such types and antitypes are identified, meaning that there are variable relationships. Another alternative base model is the *Zero Oder CFA model,* which assumes all configurations should have the same probability. Any patterns deviating from equal probability could be identified as types/antitypes. However, the majority of the literature only considers *First Order CFA model*. In this study, our focus was to examine the relationship between sun glare and collision occurrence. Thus, the *First Order CFA model* was used to calculate the expected cell frequencies. Under the assumption of independence, the expected frequencies were computed in the same manner as described in Section 4.2.2.

- The second step is to compare the observed and expected frequencies using a statistical testing. Pearson's chi-squared test, the binomial test and the hypergeometric test of Lehmacher are three most common tests in CFA. In contrast to hypergeometric test of Lehmacher, Pearson's chi-squared test and binomial test are often preferred in research because they are applicable to all CFA chance models and the Lehmacher test tends to be non-conservative when sample size is small. Mathematically, the binomial test is more powerful than Pearson's chi-squared test. This is because, for an identical difference between observed and expected frequencies tested in the two tests, the calculated statistic Z under binomial test is always larger than χ under Pearson's chi-squared test, allowing binomial test to detect more types and antitypes (Eye et al., 1996). Therefore, in this study, the binomial test was used to conduct the statistical difference test. For more information about the three tests, readers may refer to Eye et al. (1996). The standard normal approximation of the binomial test applies when most of the expected

frequencies $E_{i,j} \geq 10$, which is the case in this dataset. The binomial statistic Z is calculated as shown below.

$$Z_{ij} = \frac{O_{ij} - E_{ij}}{\sqrt{E_{ij}(1 - p_{ij})}}$$ (4-4)

$$p_{ij} = E_{ij}/N$$ (4-5)

where, O_{ij} denotes the observed frequencies; E_{ij} denotes the expected frequencies and N denotes total numbers of observations.

- The last step is to identify types and antitypes based on the *p*-value calculated from the Z statistic, which follows a standard normal distribution. In this study, type/antitypes were detected based on a confidence level of 90% and were then used to interpret the impacts of sun glare.

4.2.4. The Wilcoxon Signed-Rank Test

Since the data of the same month in the case and control groups can be considered as matched pairs controlled by the differences in sun glare exposure, the Wilcoxon Signed-Rank Test (W test) can be used to conduct a paired difference test of collision occurrence among different directions between the two weather conditions. It is an alternative to the paired *t*-test, which can be applied when the samples do not follow a normal distribution such as the collision frequencies. The goal of conducting this method is to verify whether the sun glare has adverse effects on road safety by increasing the eastbound collisions in morning glare period and westbound collisions in evening glare period. In this study, the comparison was conducted using the ratio of collisions on glare exposed direction and non-glare exposed directions between the two groups. The ratio X_i was paired for each month of the groups and can be calculated as Equation 4-6, where the glare exposed directions are termed as east in the morning and west in the evening.

$$X_i = \frac{crashes\ on\ glare\ exposed\ direction}{crashes\ on\ non-glare\ exposed\ direction}$$ (4-6)

The null hypothesis of this test is that there is no difference between the two groups of collision ratios, while the alternative hypothesis is that this kind of ratio would be higher under the occurrence of sun glare. The corresponding steps and formulas are shown below (Siegel, 1956).

Step1: Let N be the total number of pairs in the sample; X_{Ai} and X_{Bi} denotes the ratio point in the two groups: case group A and control group B. For each pair from $i = 1, ..., N$, calculate the $|X_{Ai} - X_{Bi}|$ and its sign.

Step 2: Exclude pairs with $|X_{Ai} - X_{Bi}| = 0$. Let N_r be the reduced sample size.

Step 3: Order and rank the remained pairs from 1 to N_r according their absolute difference $|X_{Ai} - X_{Bi}|$. Rank the ties by the average of the ranks they span. The rank number of each pairs are denoted as R_i.

Step 4: The test statistic is calculated as $W = \sum_{i=1}^{N_r}[sign(X_{Ai} - X_{Bi}) * R_i]$, and can be compared to a critical value from a reference table (Lowry, 2014). When the number of pairs is over 10, the sampling distribution of W converges to a normal distribution. Thus, a Z score can be applied to perform the hypothesis test. The equation of Z score is shown as below (Lowry, 2014).

$$Z = \frac{W}{\sigma_W} \qquad (4\text{-}7)$$

$$\sigma_W = \sqrt{\frac{N_r(N_r+1)(2N_r+1)}{6}} \qquad (4\text{-}8)$$

4.3. Summary

This chapter described the methodological approaches used in this study for assessing the safety effects of sun glare on road networks in the city of Edmonton. A two-stage analysis was carried out: a sun glare occurrence analysis followed by a detailed collision analysis. The first stage is a pre-processing analysis for the second stage, which simulates the sun glare exposure for the roads and is used to as the premise to extract the comparable data for collision comparison. Two steps were carried out in the first stage: identifying the potential sun glare time windows and corresponding locations. Three main factors including sun positions, angle of glare, and terrain configuration, were considered when identifying the time and locations. Consequently, the second stage carried out various statistical analyses based on the extracted collisions for the

identified time window and locations. A case-control study design was used to compare the collision data with and without sun glare. To exclude other adverse weather effects, only two weather conditions were considered with clear cloud cover representing the potential occurrence of sun glare, and overcast cloud cover presenting the non-glare condition. Based on the assembled data, three statistical techniques were proposed to analyze the difference in historical collision frequencies. The chi-square test of independence focused on the determination of the relationship between sun glare and collision occurrence, while the CFA examined whether the collision frequency along certain glare exposed direction was significantly increased due to the presence of sun glare, and thus can complement the existing evidence on the effects of sun glare on road safety more specifically. As for the Wilcoxon Signed-Rank test, it was used to further verify whether the sun glare leads to differences in collision occurrence. Detailed results of the two-stage analysis are shown and discussed in Chapter 5.

CHAPTER 5. RESULTS AND DISCUSSIONS

This chapter summarizes the results from the sun glare safety assessment. The major findings from the two-stage analysis on sun glare location identification and safety effects are discussed. In the first stage, which focused on the sun glare occurrence analysis, glare prone locations were identified for each glare period in every month. Based on the results of this analysis, the identified locations were plotted and visualized using maps in ArcGIS. The percentage of total length of road segments that had an increased risk due to sun glare was calculated and discussed. Based on these results, all the related historical collisions from 2007-2011 were extracted and analyzed in the second stage. The collision data was used to conduct rigorous statistical analyses to investigate the direct impacts of sun glare on road safety. Three collision analyses were conducted in this section i) to examine general sun glare impacts, ii) seasonal differences, and iii) effects on certain collision types. Considering the differences in driving maneuvers and behaviour, intersection and mid-block collisions were analyzed separately.

5.1. Results of the Sun Glare Occurrence Analysis

Sun glare is most potent to drivers when it is just above the horizon, and normally occurs right before or after sunrise or sunset. As described in Section 4.1.1, a series of time windows for sun glare risks were identified for both morning and evening periods of each month from February to October. Because of Edmonton's high latitude, the other three winter months (November, December and January) were analyzed separately due to them exhibiting sun glare effects throughout the entire daytime, where the sun continued to be low in the sky with an elevation angle of less than 20°. The sun exposure on the road network during these glare time widows was simulated by considering the road geometries as well as its surrounding terrain configurations. Based on the GIS road network and DEM, the locations meeting the requirements of sun glare occurrence were identified and extracted. As a result, a series of visualization maps were created for the corresponding glare prone locations for each glare time window in the ArcGIS.

Figure 5.1 shows the result of all glare prone locations during the morning glare periods from February to October. A sun glare road coverage percentage was calculated as the length of roads affected by the sun to the total length of the road network and is indicated on the top left corner of each map. As shown on the maps, the distribution of the locations that were affected by major glare were similar among the months of April, May, June, July, August, and September. These were roads with a primarily east-west orientation. This might be due to the road network in Edmonton having east-west/north-south grids, which diminish the potential differences between various months. However, such a simplified scenario is ideal for safety analyses as it would be much easier to separate collisions according to their exposure to sun glare by picking out particular glare exposed directions, such as east in the morning and west in the evening. Since certain months (May, Jun, and July) in the Summer Solstice have a longer duration of glare times, the affected locations due to sun glare were found to be slightly denser on the maps. While in the months of February and October, the sun rises from the southeast direction, which does not overlap much with the geometry of the grid network. The number of affected roads for the two months was considerably less compared to the other months of the year. Similar findings were also observed in the maps of evening glare periods, which is shown in Figure 5.2. The full-scale maps of each month are presented in Appendix A, B and C.

For three winter months, all road segments are considered to have an increased risk of sun glare during daytime, as the sun is always low in the sky. However, the certain affected areas vary as time changes during the day. To further clarify the sun glare effects in winter, the glare time periods were split according to the cardinal direction of the sun. The glare time windows of winter are shown in Table 5.1. The solar azimuth angle was broken into in four 90° orientation quadrants. The time periods with sun azimuths in the East quadrant (azimuth from 45° to 135°) were identified as the eastbound glare period (morning glare). Accordingly, southbound (daytime glare) and westbound glare period (evening glare) were also identified, respectively. For each time periods, the corresponding sun glare affected locations were also mapped and are shown in Figure 5.3. It was found that during these three winter months, the southbound glare period accounted for most parts of the daytime, which mainly affected the roads with north-south orientation. Eastbound glare period and westbound glare period were only found in January and

November. For the month of December, only a southbound glare period was detected because of the extreme position of the sun.

Table 5.1 Sun Glare Time Windows for Winter

Month	Eastbound Glare		Southbound Glare		Westbound Glare	
	Time Windows	Sun Azimuths	Time Windows	Sun Azimuths	Time Windows	Sun Azimuths
January	8:50-9:30	129.5°-135.6°	9:45-16:00	140.7°-225.3°	16:00-16:25	225.3°-230.5°
November	8:30-9:15	127.4°-137.1°	9:15-15:30	137.1°-222.6°	15:45-16:20	225.7°-232.4°
December	-	-	9:00-16:00	132.7°-226.1°	-	-

It should be noted that although the visualization maps could indicate where and when the roads are exposed to sun glare, they can only provide a general understanding of the glare occurrence in each month and cannot reflect the intensity of the glare by the seasonal variances of the sun positions. In other words, the impact of sun glare on road safety cannot be interpreted from these maps as the collision occurrence is highly influenced by many other factors. Therefore, a detailed collision analysis is conducted in the next section to further examine the extent of sun glare effects on road safety.

Coverage: 12.3%

February Morning

Coverage: 41.7%

March 15-31th Morning

Coverage: 40.6%

April Morning

Coverage: 42.1%

May Morning

Coverage: 43.6%

June Morning

Coverage: 42.7%

July Morning

Coverage: 40.1%

August Morning

Coverage: 39.5%

September Morning

Coverage: 11.9%

October Morning

Figure 5.1 Glare prone locations of morning glare periods

Coverage: 14.0%

February Evening

Coverage: 41.9%

March 15-31th Evening

Coverage: 40.0%

April Evening

Coverage: 40.5%

May Evening

Coverage: 41.4%

June Evening

Coverage: 40.4%

July Evening

Coverage: 40.2%

August Evening

Coverage: 39.6%

September Evening

Coverage: 14.4%

October Evening

Figure 5.2 Glare prone locations of evening glare periods

38
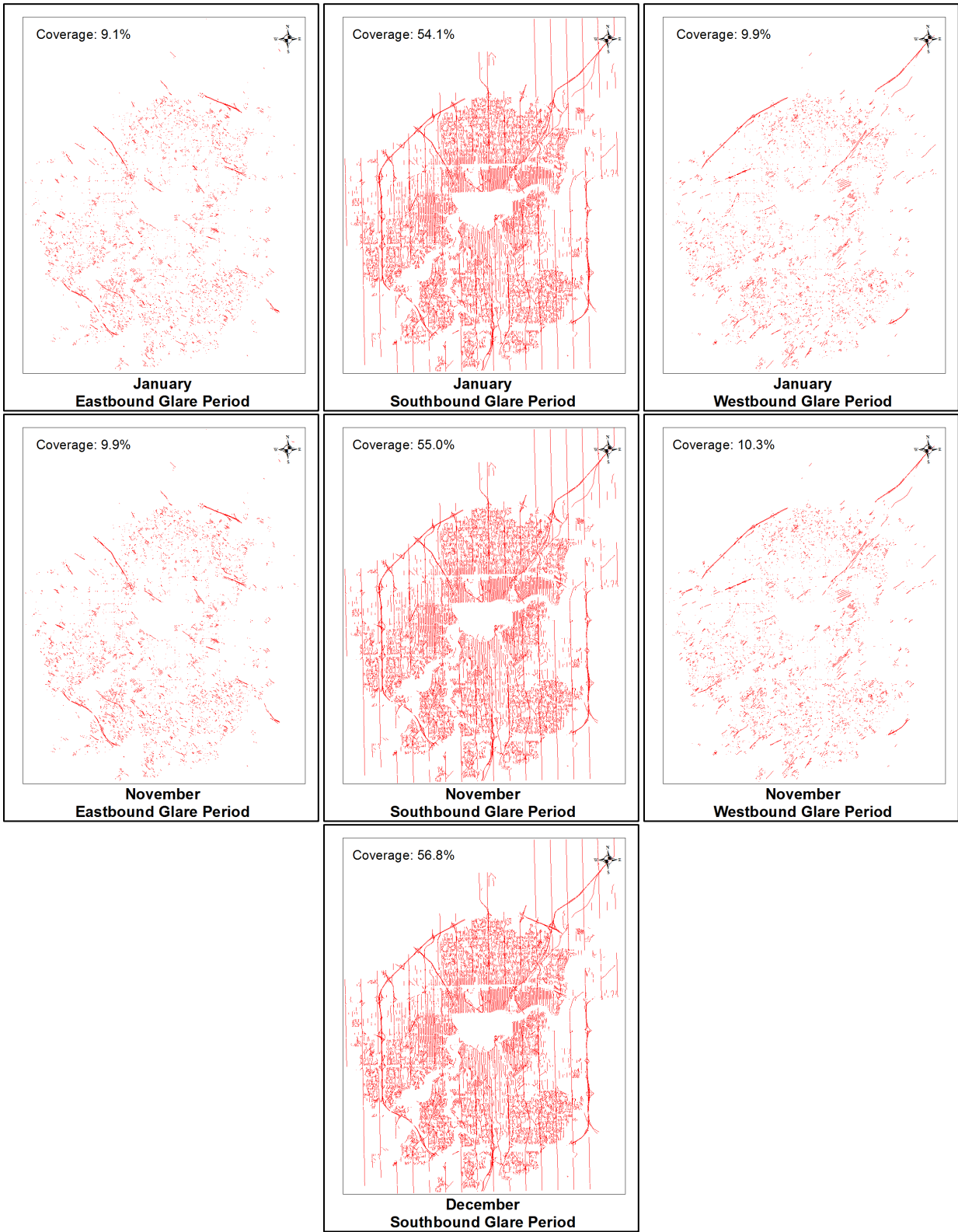
Figure 5.3 Glare prone locations of January, November and December

5.2. Assessment of Sun Glare Impacts on Collisions

The collision analysis is divided into 3 parts. The first part investigates the general effects on safety due to sun glare. The second and third parts examine the monthly variations and the effects of sun glare on certain collision types, respectively. The results of each part are discussed below.

5.2.1. *Overall Effects of Sun Glare on Collision Occurrence*

Using Tables 4.2 and 4.3, the aggregated collision data from February to October over the 5 analysis years was used to examine the general sun glare effects on road collisions. Collisions occurring in the other three winter months (November, December and January) were analyzed separately in Section 5.2.2 due to their unique sun positions. The basic hypothesis in this section was that sun glare would increase the risk of collisions in the directions exposed to sun glare on those identified glare prone locations, meaning that the number of collisions on the eastbound direction (in the morning) and westbound direction (in the evening) would be higher than other directions. To control for potential confounding factors, a control group consisting of collisions occurring during overcast weather is used as a comparison for the case group which includes collisions occurring in clear weather. The results of the three statistical techniques, as described in Chapter 4.2, are summarized in this section.

5.2.1.1. Results of the Chi-square test of independence

The Chi-square test of independence was firstly employed to determine the relationship between the sun glare and corresponding collision frequencies. The two categorical variables in the contingency table of each period were the cloud cover conditions (clear or overcast) and the collision direction (exposed to sun glare or not). If there is a significant association between these two variables and the increase of collisions falls in the directions exposed to sun glare, it can be interpreted that the sun glare has adverse impacts on the road safety. Table 5.2 and 5.3 show the results of the chi-square test of independence.

Table 5.2 Results of Chi-square Test for Overall Effects (Intersection Collisions)

Glare Periods	Group	Observed Collisions		Expected Collisions		χ^2	$P(\chi^2)$	Odds Ratio
		Exposed Direction*	Non-exposed Direction*	Exposed Direction	Non-exposed Direction			Exposed Direction $\left(\frac{a*d}{b*c}\right)$
Morning	Case	258 (a)	617 (b)	231	644	7.98	<0.01	1.340
	Control	250 (c)	799 (d)	277	772			
Evening	Case	241 (a)	718 (b)	217	742	6.27	<0.05	1.301
	Control	227 (c)	880 (d)	251	856			

*Exposed direction for intersection collisions refers to east direction in the morning and west direction in the evening. Non-exposed direction refers to the other directions in the corresponding time periods, which is west, north and south in the morning and east, north and south in the evening.

Table 5.3 Results of Chi-square Test for Overall Effects (Mid-Block Collisions)

Glare Periods	Group	Observed Collisions		Expected Collisions		χ^2	$P(\chi^2)$	Odds Ratio
		Exposed Direction*	Non-exposed Direction*	Exposed Direction	Non-exposed Direction			Exposed Direction $\left(\frac{a*d}{b*c}\right)$
Morning	Case	227 (a)	181 (b)	210	198	5.94	<0.01	1.404
	Control	200 (c)	222 (d)	217	205			
Evening	Case	132 (a)	144 (b)	128	148	0.32	0.57	1.097
	Control	152 (c)	182 (d)	155	179			

*Exposed direction for mid-block collisions refers to east direction in the morning and west direction in the evening. Non-exposed direction refers to the other directions in the corresponding time periods, which is west in the morning and east in the evening.

As can be seen from the results for intersection related collisions (Table 5.2), a statistically significant association was found in both morning and evening glare periods using a 95% confidence level. To check if sun glare has any effects or increases the collisions as hypothesized, an odds ratio, which compares the odds of exposed collisions among cases to the odds among controls, was computed using Equation 5-1 for the glare exposed directions in the intersections.

$$OR = \frac{OR_{case}}{OR_{control}} = \frac{a*d}{b*c} \qquad (5\text{-}1)$$

The meanings of variables a, b, c, d are illustrated in Table 5.2. From the observed 5 years' collision data, it was found that the odds ratios for both east direction in the morning and west direction in the evening were larger than one, meaning that the exposure to sun glare increases

the safety risk at intersections. In addition, the rate of the increase of collisions was estimated to be 34.0% on the eastbound direction during the morning and 30.1% on westbound in during the evening.

Regarding mid-block related collisions (Table 5.2), the analysis was once again repeated in the same way as described previously. It is important to note that there are only two directions for the mid-block analysis, which includes the direction facing towards the sun (glare exposed direction) and direction facing away from sun (non-glare exposed direction). The results indicate that mid-block approaches with sun glare had a significantly higher collision risk during the morning glare, approximately 40% more collisions when compared to the opposing direction, at the 95% confidence level. An increase of 9.7% was found during the evening glare; however, this change was not statistically significant.

In summary, the results of the chi-square test show that sun glare has the potential to increase collision risk and, consequently, has an adverse effect on road safety. The adverse safety impacts of sun glare were statistically significant on intersections during both morning and evening glare periods, whereas on mid-block collisions, they were only significant during the morning.

5.2.1.2.   Results of Configural Frequency Analysis

To further examine the sun glare impacts on collisions, a configural frequency analysis (CFA) was conducted in this study, which aims to compare the collisions among different travel directions for glare and non-glare conditions. The null hypothesis was that the sun glare occurrence was independent from the collision direction, meaning the collision distributions on different directions should be consistent regardless of cloud cover (i.e., clear or overcast) in the two groups of data. Therefore, if it is possible to detect a type (i.e., significantly greater number of observed collisions than expected) for the collisions on the glare exposed directions in clear weather condition, the null hypothesis is rejected and it can be concluded that the sun glare plays a significant role in increasing the collision frequencies. If an antitype is detected for the directions not exposed to sun glare in the clear weather, the findings of adverse effects of sun glare will be even stronger. The type and antitype can also be detected in the overcast weather

condition; however, this would just reflect the reversing of the results in clear weather as there are only two weather scenarios in the current CFA test. Besides, the focus of this study is to investigate the types/antitypes in the clear weather condition as the primary concern is to determine whether collision frequencies increase when the visibility is impaired by the sun. Therefore, in this study, only the CFA test results of the collisions in glare condition are discussed. The base data used in this analysis is based on the contingency tables used in Chi-square test.

The results of the intersection related collisions are shown in Table 5.4. In total, two types were detected in the case group during clear weather conditions, which corresponded to the case of sun glare occurrence. One type was found for the eastbound collisions in the morning and the other one was found for westbound collisions in the evening. Both of the two types were statistically significant at a 95% confidence level. Since the eastbound (in the morning) and westbound (in the evening) are exposed to sun glare, the significant increase in collisions detected by the CFA can be used to conclude that the sun glare has adverse effects on road safety and will significantly increase the risk of collisions.

Table 5.5 shows the results for the analysis for mid-block collisions. Only one significant type (at 90% confidence level) was found in the eastbound direction during the morning glare period. No other significant types are found. The result for the mid-block collisions is similar to that of the Chi-square test, which indicates that mid-block traffic is more likely to be affected by sun glare only during the morning period. While in the evening, collisions on mid-blocks are not significantly affected by sun glare.

Table 5.4 Results of CFA for Overall Effects (Intersection Collisions)

Glare Periods	Group	Travel Direction	Collision Frequencies		o − e	Statistics		Type/antitype
			Observed (o)	Expected (e)		z	P(z)	
Morning Glare	**Case**	East	258	231	27	1.91	0.03	type
		West	224	213	11	0.80	0.21	
		North	184	216	-32	2.27	0.01	antitype
		South	208	215	-7	0.49	0.31	
	Control	East	250	277	-27	-	-	-
		West	245	256	-11	-	-	-
		North	290	259	31	-	-	-
		South	264	257	7	-	-	-
Evening Glare	**Case**	East	262	258	4	0.24	0.40	
		West	241	217	24	1.70	0.04	type
		North	251	269	-18	1.15	0.13	
		South	205	214	-9	0.71	0.24	
	Control	East	294	298	-4	-	-	-
		West	227	251	-24	-	-	-
		North	328	311	17	-	-	-
		South	257	248	9	-	-	-

Table 5.5 Results of CFA for Overall Effects (Mid-block Collisions)

Glare Periods	Group	Travel Direction	Collision Frequencies		o − e	Statistics		Type/antitype
			Observed (o)	Expected (e)		Z	P(Z)	
Morning Glare	**Case**	East	227	210	17	1.40	0.08	type
		West	181	198	-17	1.43	0.08	antitype
	Control	East	200	217	-17	-	-	-
		West	222	205	17	-	-	-
Evening Glare	**Case**	East	144	148	-4	0.33	0.37	
		West	132	128	4	0.34	0.37	
	Control	East	182	179	3	-	-	-
		West	152	155	-3	-	-	-

5.2.1.3.   Results of the Wilcoxon Signed-Rank Test

As previously described, the Wilcoxon Signed-Rank Test is used to further check whether the sun glare has negative effects on collisions. For each month, the number of collisions occurring in clear weather was paired with that of overcast weather. Thus, a total of 18 pairs were developed to conduct the test from the 9-month data when combining both the morning and evening glare periods. The paired comparison was conducted on the ratios of collisions on glare exposed direction to non-glare exposed directions between the two groups. Intersection collisions and mid-block collisions were tested separately. Specifically, for the test of intersection, the ratio X was computed as the eastbound collisions over the other three approaches for the 9 pairs in the morning and westbound collisions over the other three approaches for the 9 pairs in the evening. While for mid-block collisions, the ratios were computed as east over west for the morning pairs

and west over east for evening 9 pairs. The result summary is shown in Table 5.6. The detailed process and corresponding values of the W-test is shown in the Appendix D.

For intersection collisions, a significant higher odds ratio X_i of collisions along glare direction was found in the case group compared to the control group, indicating that sun glare changes the relative frequencies of collisions among different directions by increasing the collision occurrence along the glare directions. As for mid-block collisions, no significant differences were found between the two groups. When intersection collision and mid-block collisions were combined, it was found that the ratio X_i was still significant higher in the case group, which supports the adverse effect of sun glare on safety in general. The result of the W-test confirms the findings of the two previous tests and also shows evidence that the sun glare increases the risk of collisions, especially at intersections.

Table 5.6 Results of the Wilcoxon Signed-Rank Test

| Collision Type | Number of Pairs | Average Glare Collision Ratio X_i | | W-statistic | Z | $P(z)$ |
		Case Group	Control Group			
Intersection Collisions	18	0.38	0.30	123	2.91	<0.01
Mid-block Collisions	18	1.10	0.99	35	0.76	0.22
Overall	36	0.74	0.64	183	1.49	<0.1

5.2.1.4.   Discussions

Similar findings were obtained from the above three statistical tests. The findings provide strong evidence that sun glare is an important contributing factor to collisions. It is found that the safety of intersection traffic is significantly affected by sun glare both in the morning and evening, while the safety of mid-block traffic seems to be only affected during the morning. The possible reason for the differences of mid-block collisions between morning and evening is that drivers are more likely to be in a hurry in the morning on workdays to get to work. Such a finding cannot be substantiated from the analysis in this study since speed information was not available. However, analysis showed that the significance of mid-block morning collisions was not as high

as intersection collisions. Hence, it can be generally concluded that the adverse effects of sun glare on intersections are greater compared to mid-blocks.

By excluding sections of the road network that are shaded (by terrain or high-rise building), the glare-prone locations were isolated and identified. The shadow maps were created to represent the general condition for each month, which might not consider the exact shadow effects at the specific moment and location of each collision. However, as Edmonton's terrain is quite flat, it can be expected that the terrain configuration will not affect the final results in any meaningful way. To further check this assumption, the collision analysis was repeated using another approximate method by removing the collisions occurring with a sun elevation less than 5° upon the calculation by Michalsky's algorithm, which aims to exclude most of shadow scenarios from the analysis. Consequently, the results were found to be consistent with the findings that were presented earlier in this thesis.

5.2.2. *Monthly Glare Collisions Analysis*

As the sun position varies across different months of a year, it is reasonable to hypothesize that vision impairment due to sun glare and its impacts on road safety among different months will also vary throughout the year. To examine this monthly variation of sun glare effects, the observed collisions data were grouped by the month and analyzed. Two types of analyses are explored in this section. One is a series of CFA tests for each month from February to October, during which the morning and evening glare periods are distinct. The other one is a separate analysis for the 3 winter months (November, December and January) when the sun is always low on the horizon throughout the daytime and the morning and evening glare periods are not distinctly separable.

5.2.2.1. Monthly analysis from February to October

A series of CFA tests were performed on the observed collisions for each month based on the comparison between clear and overcast weather in the same way as the overall analysis. Table 5.7 shows the results of intersection collisions. The glare collisions data shown in this table refer

to the collisions caused by sun glare, which are the collisions occurring on the direction exposed to sun glare in clear weather. For the morning glare period, a type was found in the month of September, which showed a significantly higher number of observed eastbound collisions at a 95% confidence level. For the evening glare period, the glare related westbound collision number was significantly higher in the month of March at a 90% confidence level. Apart from the intersection analysis, the sun glare effects on mid-blocks collision were also investigated on a monthly basis and results are shown in Table 5.8. The results indicated that March had a significantly higher number of observed collisions along the east direction in the morning glare period, while there was no significant differences detected between observed and expected collisions in the evening period.

From these results, it can be concluded that March and September are the two months that are more likely to be affected by sun glare. Since the two morning and evening glare periods for the months have the same time periods around Spring Equinox and Autumn Equinox, it can be inferred that the sun vision obstruction on Edmonton's grid road network is especially potent when the sun rises exactly in the east and sets exactly in the west. Another possible reason for this phenomenon is that the morning glare and evening glare time period in March and September overlap with the peak traffic hour, which indirectly increases the risk of collision due to increased traffic volume. The direct impact of traffic volume is not captured in this study due the absence of hourly volume data. However, through the comparison based on the case and control groups, the variation in the effects of different volume is controlled within each month's analysis. Thus, it is reasonable to conclude that the higher number of collisions in the corresponding times in March and September are attributed to sun glare.

Table 5.7 Results of CFA for Monthly Analysis (Intersection Collisions)

Glare Periods	Month	Glare Collisions		o − e	Statistics		Type/antitype
		Observed (o)	Expected (e)		z	P(z)	
Morning Glare	Feb	19	19.4	-0.4	0.00	0.50	
	Mar	28	26.6	1.4	0.30	0.38	
	Apr	26	26.9	-0.9	-0.09	0.54	
	May	22	18.2	3.8	0.99	0.16	
	Jun	20	16.6	3.4	0.86	0.20	
	Jul	24	21.7	2.3	0.52	0.30	
	Aug	31	26.7	4.3	1.00	0.16	
	Sep	72	60.4	11.6	1.64	0.05	type
	Oct	15	13.7	1.3	0.26	0.40	
Evening Glare	Feb	46	43.6	2.4	0.46	0.32	
	Mar	28	20.9	7.1	1.60	0.05	type
	Apr	15	14.3	0.7	0.34	0.37	
	May	13	11.1	1.9	0.70	0.24	
	Jun	12	12.1	-0.1	0.04	0.48	
	Jul	26	26.6	-0.6	-0.13	0.55	
	Aug	21	21.8	-0.8	-0.25	0.60	
	Sep	54	46.1	7.9	1.22	0.11	
	Oct	25	26.5	-1.5	-0.27	0.61	

Table 5.8 Results of CFA for Monthly Analysis (Mid-block Collisions)

Glare Periods	Month	Glare Collisions		o − e	Statistics		Type/antitype
		Observed (o)	Expected (e)		z	P(z)	
Morning Glare	Feb	12	12.4	-0.4	-0.14	0.56	
	Mar	41	34.1	6.9	1.37	0.09	type
	Apr	29	28.1	0.9	0.28	0.39	
	May	22	19.6	2.4	0.51	0.31	
	Jun	16	14.7	1.3	0.43	0.33	
	Jul	19	22.2	-3.2	-0.84	0.80	
	Aug	25	20.8	4.2	0.98	0.16	
	Sep	61	54.4	6.6	1.03	0.15	
	Oct	3	3.7	-0.7	-0.41	0.66	
Evening Glare	Feb	15	15.0	0	-0.11	0.55	
	Mar	16	18.0	-2	-0.45	0.67	
	Apr	6	6.4	-0.4	0.02	0.49	
	May	13	12.3	0.7	0.23	0.41	
	Jun	6	7.8	-1.8	-0.77	0.78	
	Jul	20	15.1	4.9	1.38	0.08	
	Aug	13	14.8	-1.8	-0.67	0.75	
	Sep	30	28.3	1.7	0.37	0.36	
	Oct	13	12.8	0.2	0.20	0.42	

5.2.2.2. Monthly analysis for the winter

For the winter monthly analysis, the numbers of collisions were counted during each winter glare time windows as previously defined in Table 5.1. Afterwards, the winter glare effect was examined using CFA for the three defined glare periods (eastbound glare period and southbound glare period and northbound glare period). The collision data of each glare period category

consists of the aggregated data from the three months with same glare period category. The odds ratios of collisions along different directions were also computed by comparing the glare and non-glare conditions based on Equation 5-1.

The result summary for intersection collisions are shown in Table 5.9. The southbound collisions during the southbound glare period were found to be statistically significant higher than expected numbers (type at 95% confidence level) in the three months. The corresponding odds ratio was calculated to be 1.23, which indicates that the southbound collisions were increased by 23% when sun glare occurs from that direction. More than expected numbers of intersection collisions were also recorded in clear weather along the east and west directions during the eastbound and westbound glare periods, respectively. However, these two differences were not statistically significant. This could be attributed to the small sample size in these two periods. Table 5.10 shows the results for mid-block collisions. Since the number of observations was too few in the eastbound glare period and westbound glare period, the CFA was not conducted for these two periods. Only the result for southbound glare period is presented in the table. Similar to previous tests, no significant type was detected for any directions.

Table 5.9 Results of CFA in the 3 Winter Months (Intersection Collisions)

Glare Periods	Existing Months	Travel Direction	Collisions in Clear Weather		$o - e$	Statistics		Type/ antitype	Odds Ratio
			Observed (o)	Expected (e)		z	P(z)		
Eastbound Glare	Jan; Nov	East	27	22	5	1.22	0.11		1.72
		West	19	20	-1	-0.14	0.56		0.94
		North	17	20	-3	-0.70	0.76		0.72
		South	15	17	-2	-0.47	0.68		0.80
Southbound Glare	Jan; Nov; Dec	East	313	322	-9	-0.49	0.69		0.94
		West	302	309	-7	-0.46	0.68		0.90
		North	318	332	-14	-0.82	0.79		0.90
		South	372	342	30	1.73	0.04	type	1.23
Westbound Glare	Jan; Nov	East	20	17	3	0.64	0.26		1.34
		West	22	19	3	0.99	0.16		1.56
		North	13	17	-4	-1.04	0.85		0.60
		South	13	15	-2	-0.66	0.75		0.72

Table 5.10 Results of CFA in the 3 Winter Months (Mid-block Collisions)

Glare Periods	Existing Months	Travel Direction	Collisions in Clear Weather		$o - e$	Statistics		Type/ antitype	Odds Ratio
			Observed (o)	Expected (e)		z	P(z)		
Southbound Glare	Jan; Nov; Dec	North	194	196	-2	-0.14	0.56		0.96
		South	132	130	2	0.16	0.44		1.04

5.2.3. Safety Analysis on Different Collision Types

Although the above results showed that sun glare had a general adverse effect on the road safety, it is important to examine what types of collisions are over-presented due to sun glare vision impairment. Therefore, a CFA test was also conducted in this study to determine the variation of the sun glare effects among different collision types. The number of collisions was counted and aggregated according to its collision type. In this analysis, the collisions along the glare exposed direction in clear weather was used as the case group, referred as glare collisions, while the collisions occurring on the same direction in overcast weather was set as the control group and referred as the non-glare related collisions. The null hypothesis was that there was no difference in the portion of certain collision type between glare and non-glare conditions. Under this null hypothesis, the expected collisions of each type can be calculated. For both intersection and mid-block collisions, the data of morning and evening glare periods were combined and analyzed together.

Results of intersection collisions analysis are shown in Table 5.11. It was found that the collisions with the occurrence of traffic signal violations and stop sign violations were significantly higher (at 95% confidence level) than expected in the glare condition. This may well happen when the sun light is scattered in the eye and reduces the visibility of such signals and signs. Besides, pedestrian and cyclist related collisions were also found significant higher (95% confidence level) than expected under the condition of sun glare, which is consistent with the finding of previous research (Hagita & Mori, 2014). As for mid-block related collisions, Table 5.12 shows the results and indicates that the collision maneuver of improper turn and improper lane change are significantly increased by the sun glare (95% confidence level). Also animal-related collisions were significantly higher when drivers were affected by sun glare. Thus, from these findings, it can be concluded that the sun glare effect on collisions varies with different collision maneuver types. Its adverse effects are significantly potent on collisions that are related to signal violations and vulnerable road users at intersection and collision maneuvers related to improper lane changing on mid-blocks.

Table 5.11 Results of Sun glare Effects over Different Collision Types (Intersection Collisions)

Collision Maneuver Type	Glare Collisions		z	Type/ antitype	Non-glare Collisions		z	Type/ antitype
	Observed (o)	Expected (e)			Observed (o)	Expected (e)		
Back unsafely	5	7.4	-1.35		9	7.1	1.36	
Fail to yield cyclist	7	4.3	2.05	T*	1	4.1	2.07	A*
Fail to yield pedestrian	22	17.2	2.68	T*	12	16.4	-2.7	A*
Fail to yield right of way	3	2.6	0.37		2	2.4	0.37	
Flow too closely	241	250.6	3.51	A*	249	239.4	3.53	T*
Improper lane change	29	28.9	0.16		27	27.6	0.16	
Improper turn	9	9.1	-0.1		9	8.7	0.1	
Left of center	3	3.1	0.05		3	2.9	0.06	
Left turn cross path	51	52.7	0.77		52	50.3	0.77	
Ran off road	17	14.9	1.26		12	14.2	1.28	
Signal Violation	45	40.5	2.03	T*	34	38.7	2.05	A*
Stop sign violation	46	41.9	1.94	T*	36	40.1	1.96	A*
Strike parked vehicle	4	4.4	0.61		5	4.2	0.61	
Yield sign violation	15	17.3	-1.33		19	16.6	1.34	
Other	3	4.6	-1.18		6	4.4	1.19	

*significant at 95% confidence level.

Table 5.12 Results of Sun glare Effects over Different Collision Types (Mid-block Collisions)

Collision Maneuver Type	Glare Collisions		z	Type/ antitype	Non-glare Collisions		z	Type/ antitype
	Observed (o)	Expected (e)			Observed (o)	Expected (e)		
Animal action	4	2	1.72	T*	0	2	-1.73	A*
Back unsafely	6	12.3	3.83	A*	19	12.3	3.85	T*
Fail to yield pedestrian	2	1.2	0.22		1	1.2	0.23	
Fail to yield right of way	18	18.7	0.92		20	18.7	0.93	
Flow too closely	132	131.2	0.93		134	131.2	0.93	
Improper lane change	60	54.4	1.98	T*	50	54.4	1.99	A*
Improper turn	7	3.5	2.69	T*	0	3.5	-2.7	A*
Left of center	13	11.9	0.53		11	11.9	0.53	
Strike parked vehicle	80	76.7	0.67		75	76.7	0.67	
Run off road	27	28.6	1.27		31	28.6	1.27	
Other	11	10.4	0.24		10	10.4	0.24	

*significant at 95% confidence level.

5.3. Summary

The chapter describes the safety assessment results due to sun glare effects. Two stages of analysis were conducted based on the road network in Edmonton. In the first stage, the potential sun glare time windows were identified for each month and the corresponding glare-prone locations were plotted using visualization maps. It was found that the majority of locations affected by morning and evening sun glare consist of the roads with east-west orientation in the grids type road network. Furthermore, during the winter months of November, December and January, the sun glare was expected to occur throughout the entire day because of the high

latitude of Edmonton and continuous low elevation of the sun. These maps provide a reference of the glare prone locations and were used to extract glare related collisions and non-glare comparison collisions for the second stage analysis. Based on these collisions, several statistical techniques were applied to check whether sun glare is a contributing factor to collision occurrences.

The collision analysis was conducted in three parts. First, the general effects of sun glare were examined by performing the Chi-square test of independence, CFA, and *W*-test. Similar findings were obtained from all three tests, which showed that sun glare significantly contributes to collision occurrence. This adverse effect was significant on intersections both in the morning and evening periods, while the mid-block glare collisions were only found to be significantly higher in the morning glare period. Second, the CFA was performed for each month and during the winter period. The results show that vision obstruction due to glare during morning and evening periods was especially potent during spring and fall. While during most of the winter glare times traffic safety in the southbound direction was significantly affected by sun glare. Last, the CFA was also performed to check whether sun glare effect various collision types. It was found that there was a higher portion of collisions due to signal or sign violation and failing to yield to pedestrians or cyclists at intersections, while there were higher portions of collisions due to improper turn or lane change on mid-blocks.

CHAPTER 6.   CONCLUSIONS AND DISCUSSIONS

This chapter provides an overview of the research presented herein and summarizes the major findings of the pervious chapters. The contributions as well as the limitations of this research are also discussed in this chapter along with the recommendations for future work.

6.1. Research Overview

This research conducted a road safety assessment due to sun glare effects within the city of Edmonton. The overall objective was to develop a better understanding of the risks on the road network posed by sun glare. To achieve this objective, a two-stage analysis was conducted in this research, which is sun glare occurrence analysis and glare related collision analysis. The focus of the sun glare occurrence analysis was to investigate when and where sun glare occurs. While the focus of the collision analysis was to examine the direct impacts of sun glare on safety by examining historical collisions based on those identified locations and time windows with sun glare presence.

In the glare occurrence analyses presented in Sections 4.1 and 5.1, the sun glare exposure was modeled for the whole road network by considering factors associated with sun positions, the angle of the glare, the geometry of the roadway alignments, and the terrain configuration. Specifically, the glare time windows were first computed for each month based on the elevation angle of the sun, which determines whether the sunlight falls in the driver's gaze from a vertical geometrical perspective. Based on these time windows, the bearings of the roadways were then compared and matched with the corresponding sun azimuth, which determines whether the sunlight falls in the driver's gaze from a horizontal geometrical perspective. With these two steps, the sun glare risk locations during each glare time window were identified. To address the effects of the surrounding terrain configuration, which may block the sunlight at a certain angle, the hill shade tool in ArcGIS was introduced in this research to calculate the illumination for the whole road network based on the surface elevation information from a Digital Elevation Model of the city. As a result, only the roadways with direct sun exposure remained and the roads within

shadows were excluded from the analysis. Ultimately, the sun glare time windows were summarized and the corresponding locations were plotted in a series of visualization maps, which can be used as a reference for the public to know when and where there is a risk of sun glare.

For the collision analyses presented in Sections 4.2 and 5.2, the glare related collisions based on the identified locations and time windows were extracted as well as a control dataset for comparison was assembled. The collision analysis was based on the comparison between collisions on the same locations and time of day, but under different weather conditions (clear vs. overcast). With the exception of the presence of sun glare exposure, which is controlled by the weather condition, the control group is comparable to the case group in every possible way. Therefore, it can be expected that the differences of the compared collisions are caused by the exposure to the sun glare and not due to any other factors.

In total, three major research questions were addressed - 1) whether the sun glare has adverse effects on road safety in general, 2) whether the sun glare effect is consistent for different months over a year, and 3) what types of collisions are over-presented due to sun glare vision obstruction. To test the significance of the collision differences, three statistical techniques were employed and included: chi-square test of independence, configural frequency analysis, and the Wilcoxon signed rank test. The major findings are summarized in the following section.

6.2. Research Findings

In the glare occurrence analysis, the sun glare was found to usually occur right after-and-before sun rise and sun set. Accordingly, two kinds of glare time periods (morning and evening) were identified for the months of February to October over a typical year. As most parts of the road network in Edmonton are arranged in typical east-west/north-south grids, the distributions of the identified locations on the map during morning and evening glare periods were quite similar among most of the months and consisted of the roads with east-west orientation. The coverage of sun glare affected roads in these two glare periods accounted for about 40% of the total road network length, with two exceptions being the months of February and October, which only had

a coverage percentage from 11.9% to 14.4%. As for the other three months in winter, the sun glare was found to occur throughout the entire daytime as the sun was continuously low on the horizon. The affected areas varied as time changed during the day. However, it was found that during most of the glare times in winter, the sun was located in the south direction, meaning that the majority of exposed roads were those with north-south orientation.

In the collision analysis, the collisions counts were compared between glare condition and non-glare condition by controlling for other confounding factors. Three research questions were addressed in this analysis. First, sun glare was found to have significant adverse impacts on road safety in general. Similar findings were obtained from several statistical tests and showed that the sun glare significantly contributes to collision occurrence, especially at intersection. Quantitatively, the collisions were estimated to increase by approximately 30% during sun glare times. Second, evidence from the monthly analysis showed that sun glare effects in the morning and evening periods were especially potent in the months of spring and fall. While in most of the daytime in January, November and December, the traffic safety in the southbound direction was significantly affected by the sun glare. Lastly, certain collision maneuver types were over-presented than others under the influence of sun glare. It was found that collisions related to signal violations and failing to yield to pedestrians and cyclist were over-presented at intersections. At mid-block locations, the proportion of collisions due to improper turn and lane change were found to be significantly higher.

6.3. Research Contributions

There are three major contributions in this research.

- This research develops a general knowledge regarding the effects of sun glare using the city of Edmonton as a case study. The key factors that determine sun glare conditions are demonstrated and a sunlight exposure modeling methodology is proposed to identify when and where road users are going to be vulnerable to sun glare. This research can be used to assist in alleviating the risks associated with sun glare in the planning and designing of future roads.

- The sun glare exposure modeling was linked with a glare related collision analysis. By identifying the specific sun glare prone locations and examining their corresponding historical collisions, this research helps to provide additional insights about the extent by which sun glare affects road safety.

- The safety assessment of the sun glare effects is conducted using a large sample size on a city-wide scope. By controlling for several confounding factors such as weather condition, collision time/location, and travel direction that would change collision occurrence, the safety risk posed by sun glare are thoroughly examined from different aspects, including overall effects, monthly analysis, and collision maneuver variation.

6.4. Research Limitations and Recommendations for Future Work

As with any research, there are a few limitations that may be addressed as part of future work.

First, the safety assessment can be improved by analyzing the differences of sun glare effects on different road environments. Other important collision exposure information may be collected and incorporated into the analysis such as traffic volume, the number of lanes and the average speeds.

Second, due to the lack of detailed elevation models of the buildings and other surrounding objects available for use, the shadow effects are only addressed by considering the terrain configuration of the surface and excluding the downtown area where a majority of high-rise buildings are dominantly present. This may be improved if a more detailed digital elevation model can be obtained and a more precise shadow coverage maps can be generated.

Last, as the sun glare is a spatial-temporal factor, which makes difficult to capture its exact relation to a collision, the safety impacts assessment may be improved if more information of the glare presence can be recorded in the collision reports. Besides, as the cloud cover also plays an important role on where sun glare occurs, future works may be carried out to improve the modeling of cloud cover for sun glare.

REFERENCES

Andrey, J., Mills, B., & Vandermolen, J. (2001). Weather information and road safety. *Institute for Catastrophic Loss Reduction, Toronto, Ontario, Canada*.

Auffray, B., Monsere, C. M., & Bertini, R. L. (2008). An empirical investigation of the impacts of sun-related glare on traffic flow. In *Proc., 87th Annual Meeting of Transportation Research Board*. Transportation Research Board Washington, DC.

Ayres, T. J., Kelkar, R., & Woodruff, W. H. (2004). Driver adjustment to solar glare. *Proceedings of the Human Factors and Ergonomics Society Annual Meeting*, *48*(19), 2295–2299. https://doi.org/10.1177/154193120404801919

Babizhayev, M. A. (2003). Glare disability and driving safety. *Ophthalmic Research*, *35*(1), 19–25. https://doi.org/10.1159/000068199

Choi, E.-H., & Singh, S. (2005). Statistical assessment of the glare issue-human and natural elements. *National Center for Statistics and Analysis*.

Churchill, A. M., Tripodis, Y., & Lovell, D. J. (2012). Sun glare impacts on freeway congestion: geometric model and empirical analysis. *Journal of Transportation Engineering*, *138*(10), 1196–1204.

Daniel, J. R., & Chien, S. I. (2009). Impact of adverse weather on freeway speeds and flows. Presented at the Transportation Research Board 88th Annual MeetingTransportation Research Board, Washington, D.C. Retrieved from https://trid.trb.org/view.aspx?id=881946

Environment Canada. (2013, April 16). Weather information - Environment Canada. Retrieved June 17, 2017, from https://weather.gc.ca/index_e.html

ERSI. (n.d.). Split line at vertices (data management). Retrieved July 7, 2017, from http://resources.esri.com/help/9.3/arcgisengine/java/gp_toolref/data_management_tools/split_line_at_vertices_data_management_.htm

ESRI. (2016). About esri : the science of where. Retrieved July 6, 2017, from http://www.esri.com/about-esri#what-we-do

Eye, A., Spiel, C., & Wood, P. K. (1996). Configural frequency analysis in applied psychological research. *Applied Psychology*, *45*(4), 301–327.

Grena, R. (2008). An algorithm for the computation of the solar position. *Solar Energy*, *82*(5), 462–470. https://doi.org/10.1016/j.solener.2007.10.001

Hagita, K., & Mori, K. (2013). The effect of sun glare on traffic accidents in Japan. Presented at the Transportation Research Board 92nd Annual MeetingTransportation Research Board. Retrieved from https://trid.trb.org/view.aspx?id=1241470

Hagita, K., & Mori, K. (2014). The effect of sun glare on traffic accidents in Chiba prefecture, Japan. *Asian Transport Studies*, *3*(2), 205–219. https://doi.org/10.11175/eastsats.3.205

Hermans, E., Brijs, T., Stiers, T., & Offermans, C. (2006). The impact of weather conditions on road safety investigated on an hourly basis. Retrieved from https://uhdspace.uhasselt.be/dspace/handle/1942/1365

Jurado-Pina, R., & Pardillo-Mayora, J. M. (2010). Methodology to analyze sun glare impact on highway under prolonged exposure. *Journal of Transportation Engineering*, *136*(12), 1137–1144.

Khumalo, N. (2014). *Visibility improvements through information provision regarding sun glare : a case study in Cape Town* (Thesis). University of Cape Town. Retrieved from https://open.uct.ac.za/handle/11427/13307

Lowry, R. (Richard). (2014, April). Concepts and applications of inferential statistics. Retrieved June 18, 2017, from http://vassarstats.net/textbook/ch12a.html

Massey, R. (2013, October 16). Glare of the sun contributes to 3,000 road accidents and is particularly dangerous this time of year. Retrieved July 6, 2017, from http://www.dailymail.co.uk/news/article-2461972/Glare-sun-contributes-3-000-road-accidents-particularly-dangerous-time-year.html

McGwin, G., Chapman, V., & Owsley, C. (2000). Visual risk factors for driving difficulty among older drivers. *Accident Analysis & Prevention*, *32*(6), 735–744.

Michalsky, J. J. (1988). The Astronomical Almanac's algorithm for approximate solar position (1950–2050). *Solar Energy*, *40*(3), 227–235. https://doi.org/10.1016/0038-092X(88)90045-X

Mitra, S. (2014). Sun glare and road safety: An empirical investigation of intersection crashes. *Safety Science*, *70*, 246–254. https://doi.org/10.1016/j.ssci.2014.06.005

Ranney, T. A., Simmons, L. A., & Masalonis, A. J. (1999). Prolonged exposure to glare and driving time: effects on performance in a driving simulator. *Accident; Analysis and Prevention*, *31*(6), 601–610.

Schreuder, D. A. (1968). Side lights and low-beam headlights in built-uo areas. Retrieved from https://trid.trb.org/view.aspx?id=109187

Shapefiles: ArcGIS online help. (n.d.). Retrieved July 6, 2017, from http://doc.arcgis.com/en/arcgis-online/reference/shapefiles.htm

Shepard, F. D. (1996). *Reduced visibility due to fog on the highway*. Transportation Research Board.

Siegel, S. (1956). *Nonparametric statistics for the behavioral sciences*. McGraw-Hill.

Staver, J. (2015, May 4). Sun glare accidents. Retrieved July 6, 2017, from https://www.chicagolawyer.com/sun-glare-accidents/

Theeuwes, J., Alferdinck, J. W., & Perel, M. (2002). Relation between glare and driving performance. *Human Factors*, *44*(1), 95–107.

Walraven, R. (1978). Calculating the position of the sun. *Solar Energy*, *20*(5), 393–397. https://doi.org/10.1016/0038-092X(78)90155-X

Wood, J. M., & Owens, D. A. (2005). Standard measures of visual acuity do not predict drivers' recognition performance under day or night conditions. *Optometry and Vision Science*, *82*(8), 698–705.

Zwahlen, H. T. (1989). Conspicuity of suprathreshold reflective targets in a driver's peripheral visual field at night. *Transportation Research Record*, (1213).

# APPENDIX A. GLARE PRONE LOCA-TIONS OF MORNING GLARE PERIODS

Coverage: 12.3%
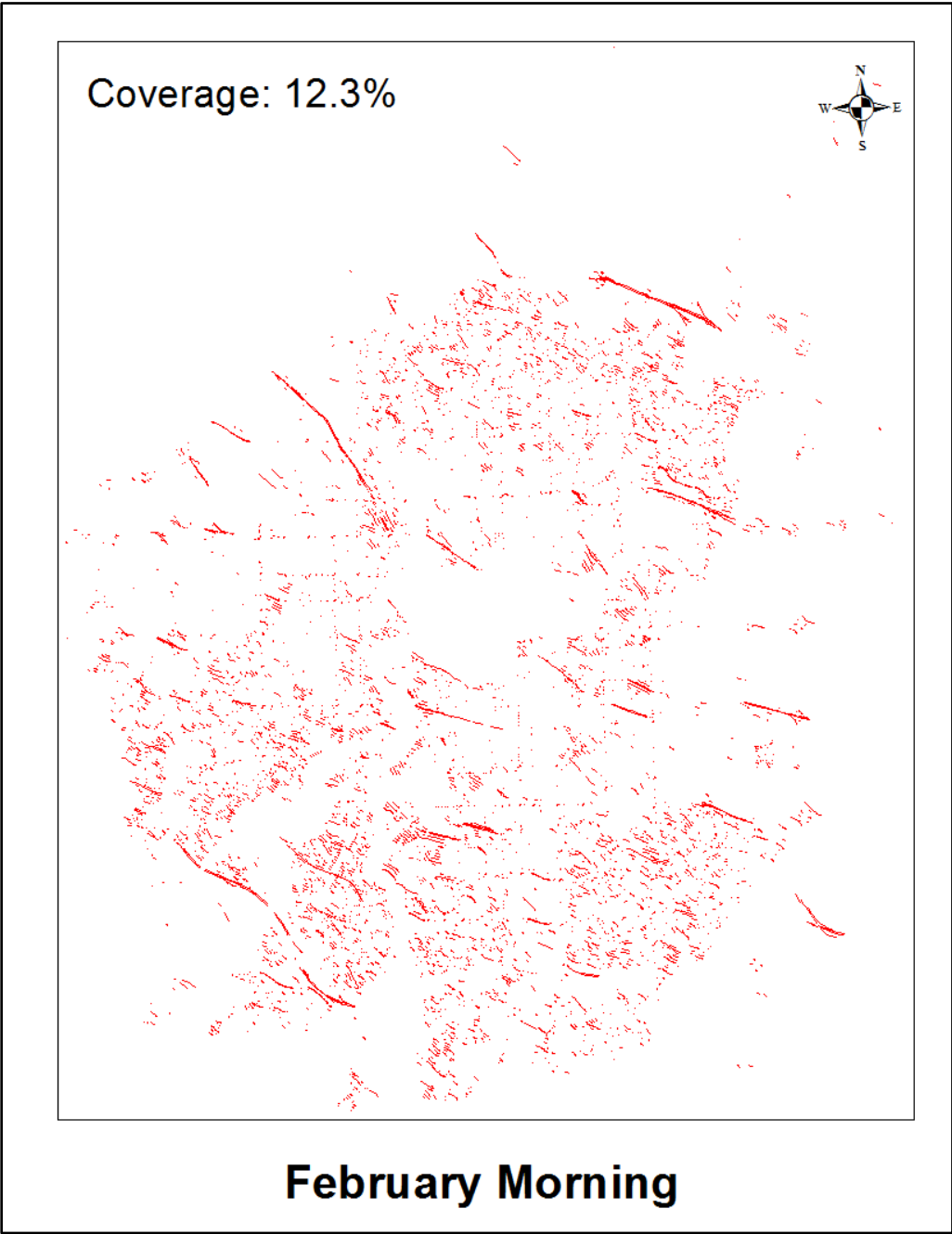
February Morning

Figure A. 1 Glare prone locations of morning glare period in February
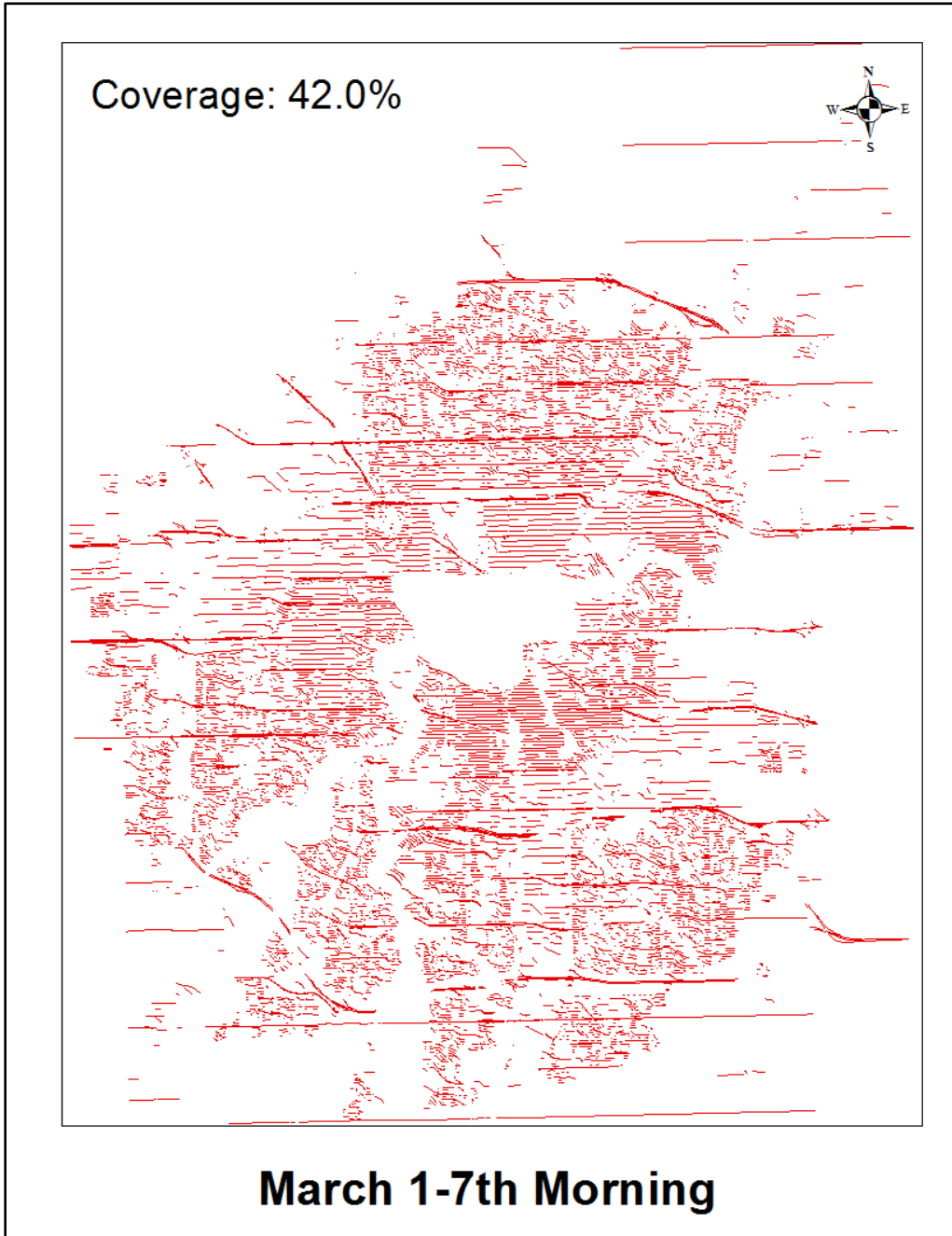
Figure A. 2 Glare prone locations of morning glare period in March 1-7th

Coverage: 41.7%

March 15-31th Morning

Figure A. 3 Glare prone locations of morning glare period in March 15-31th
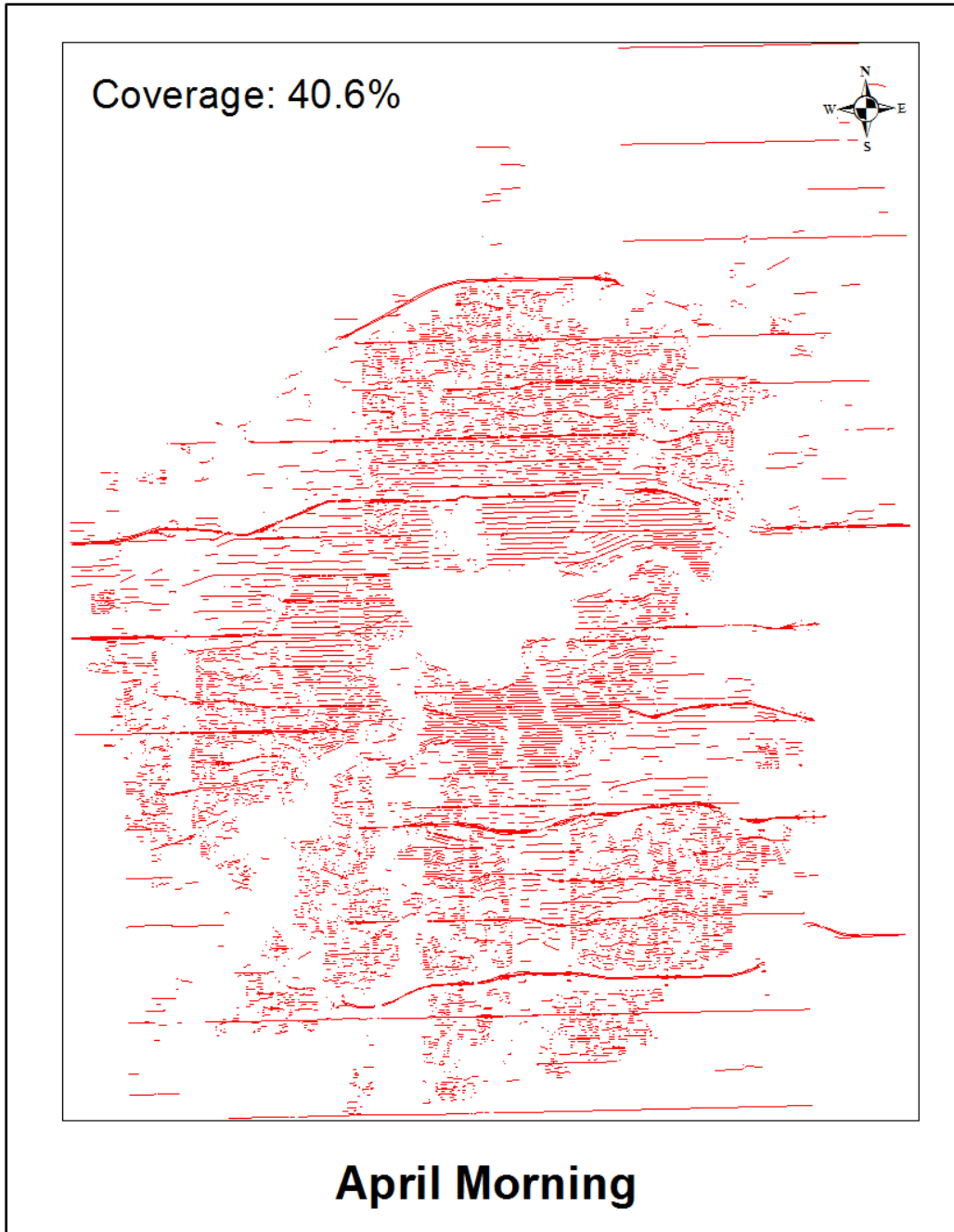
**Figure A. 4 Glare prone locations of morning glare period in April**

May Morning

Figure A. 5 Glare prone locations of morning glare period in May

Figure A. 6 Glare prone locations of morning glare period in June

**Figure A. 7 Glare prone locations of morning glare period in July**

Coverage: 40.1%
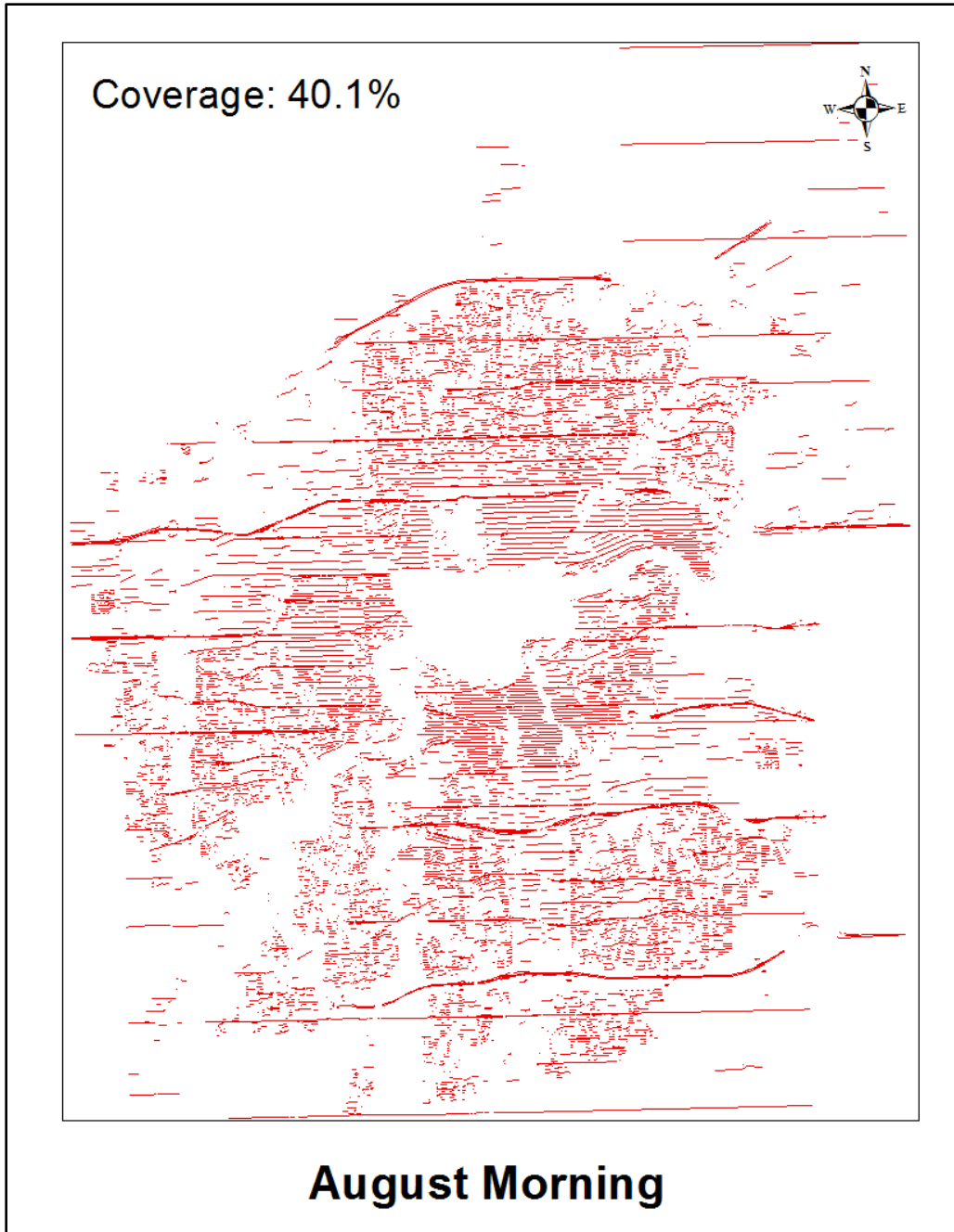
August Morning

Figure A. 8 Glare prone locations of morning glare period in August
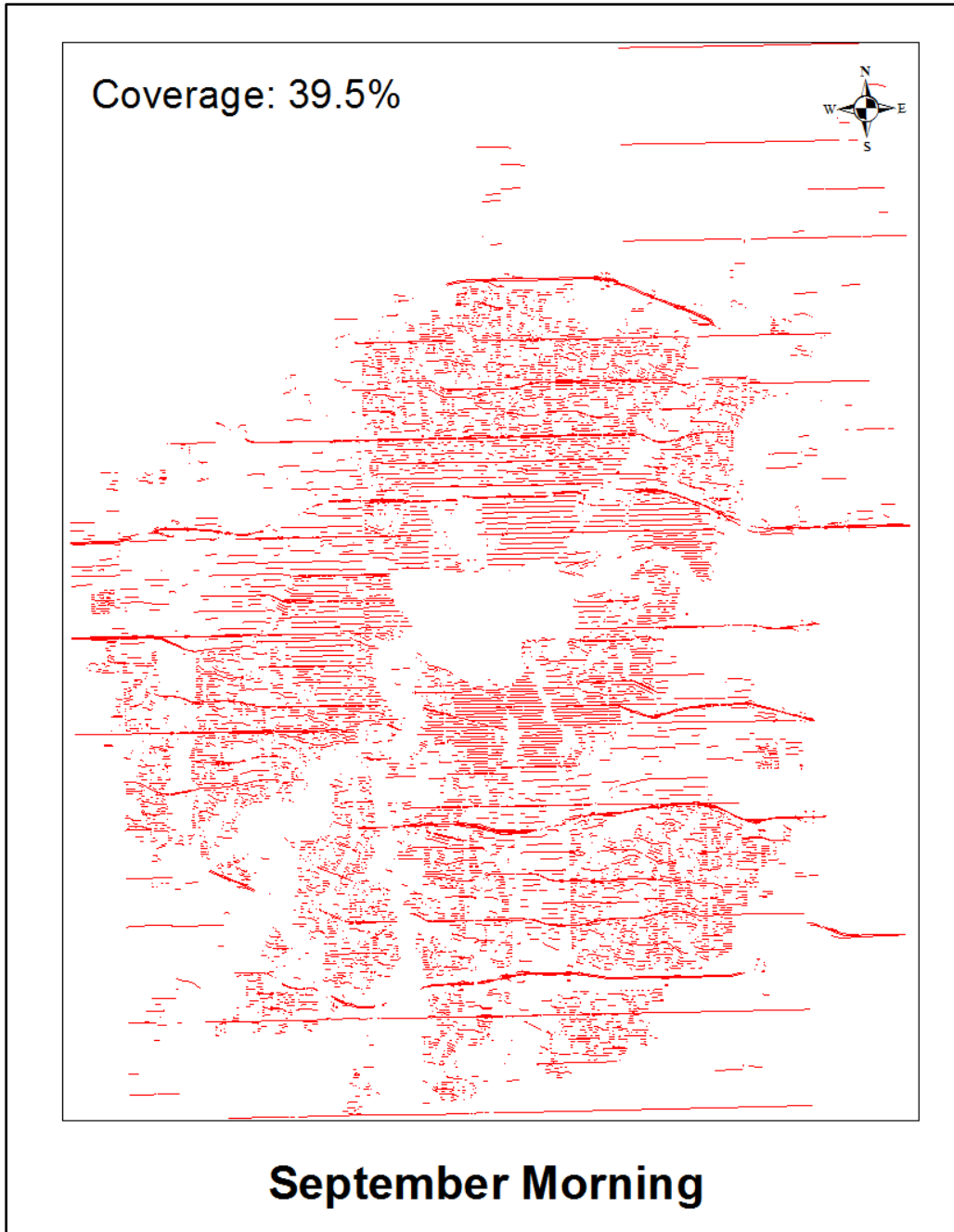
Figure A. 9 Glare prone locations of morning glare period in September

Coverage: 11.9%
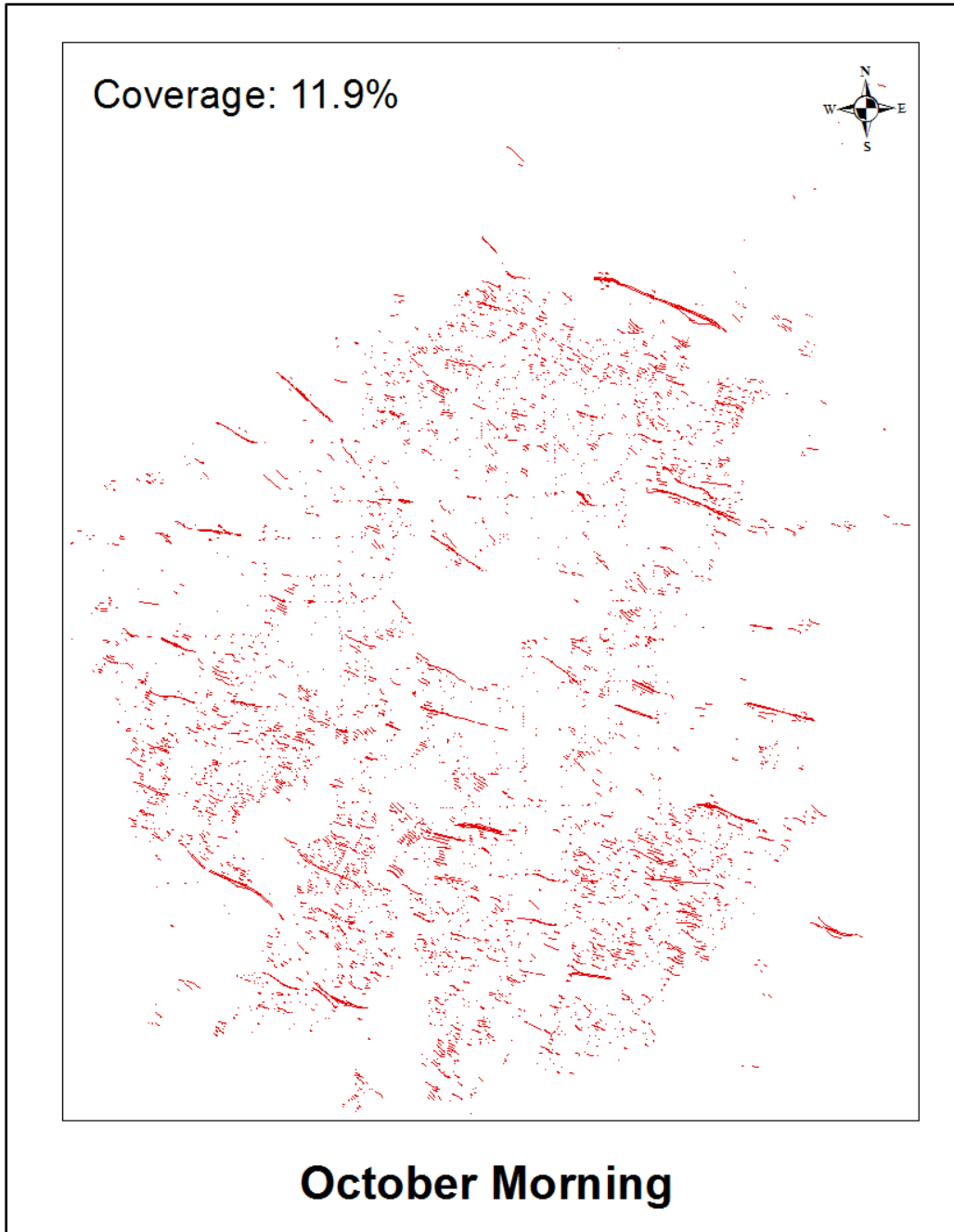
October Morning

Figure A. 10 Glare prone locations of morning glare period in October

APPENDIX B. GLARE PRONE LOCATIONS OF EVENING GLARE PERIODS
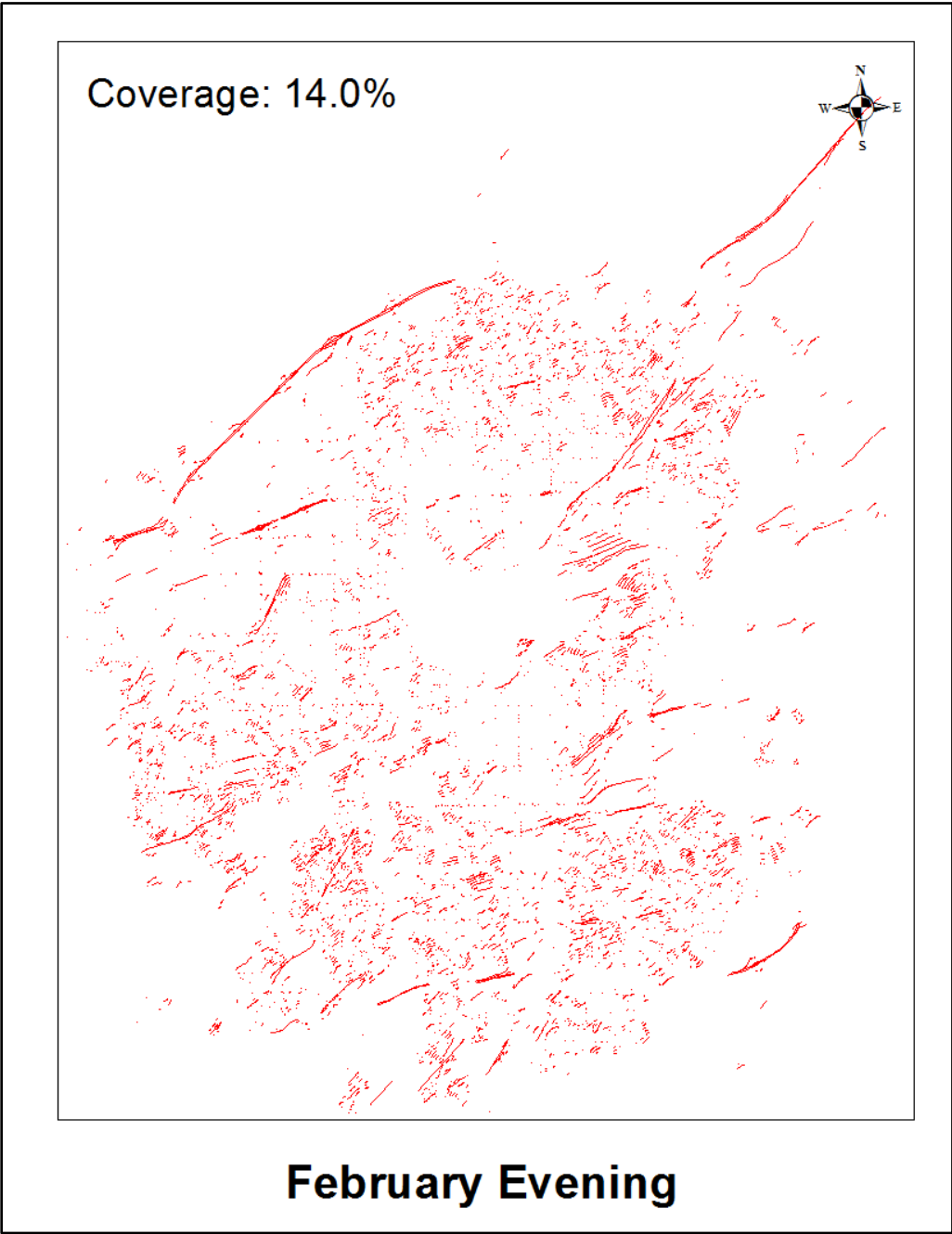
Figure B. 11 Glare prone locations of morning glare period in February

Coverage: 43.6%

March 1-7th Evening
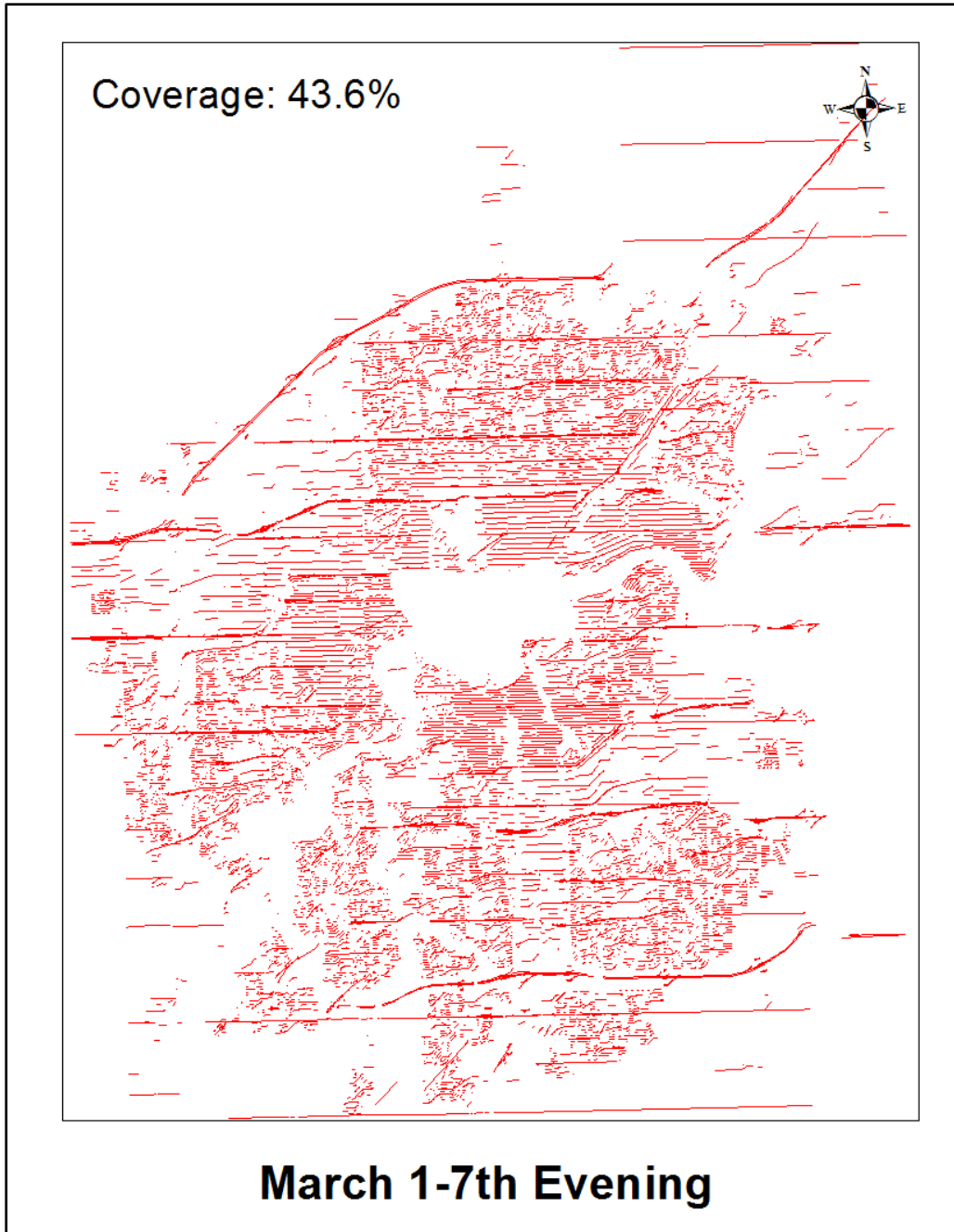
**Figure B. 2 Glare prone locations of morning glare period in March 1-7th**

Figure B. 3 Glare prone locations of morning glare period in March 15-31th
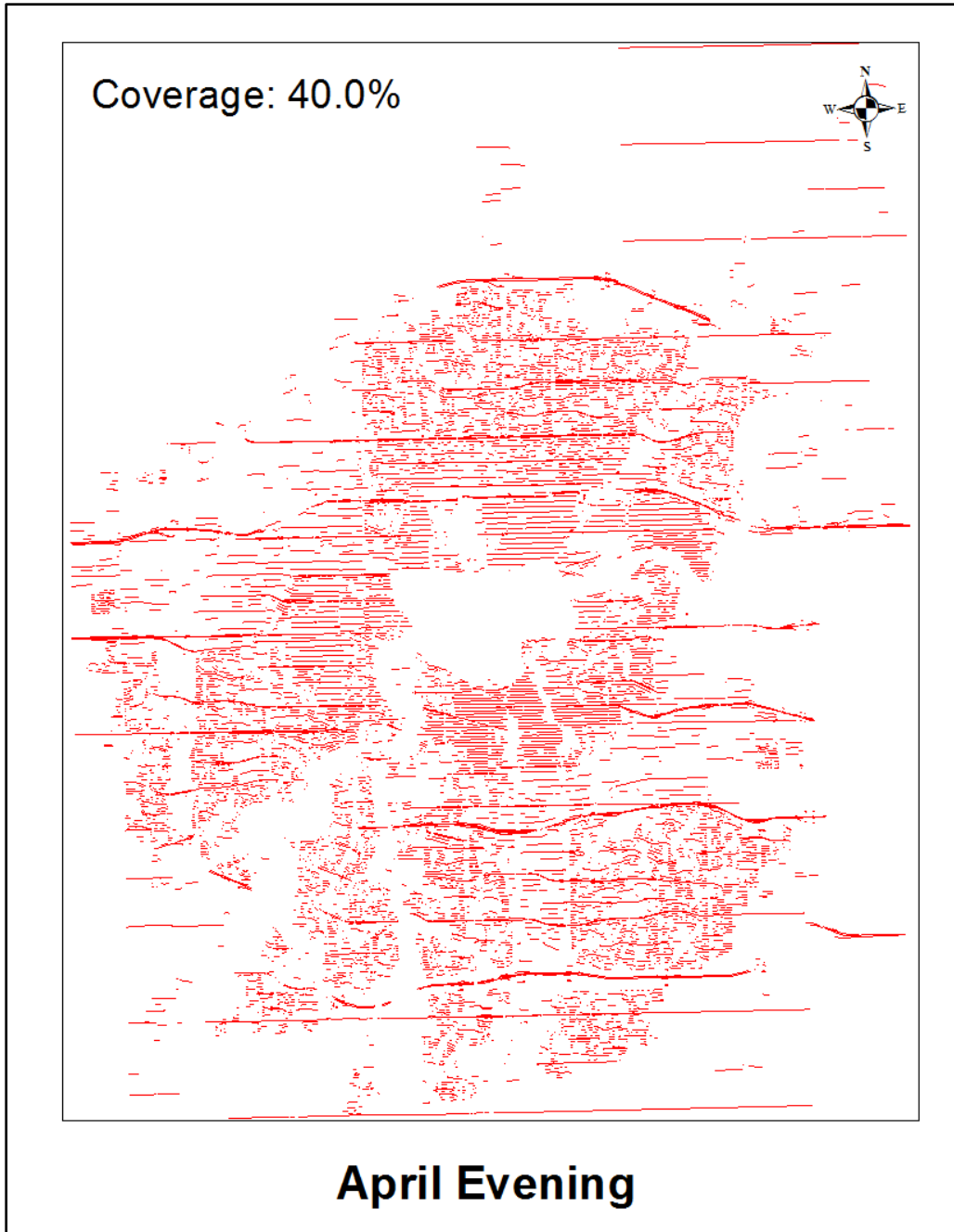
Figure B. 4 Glare prone locations of morning glare period in April

Coverage: 40.5%

May Evening
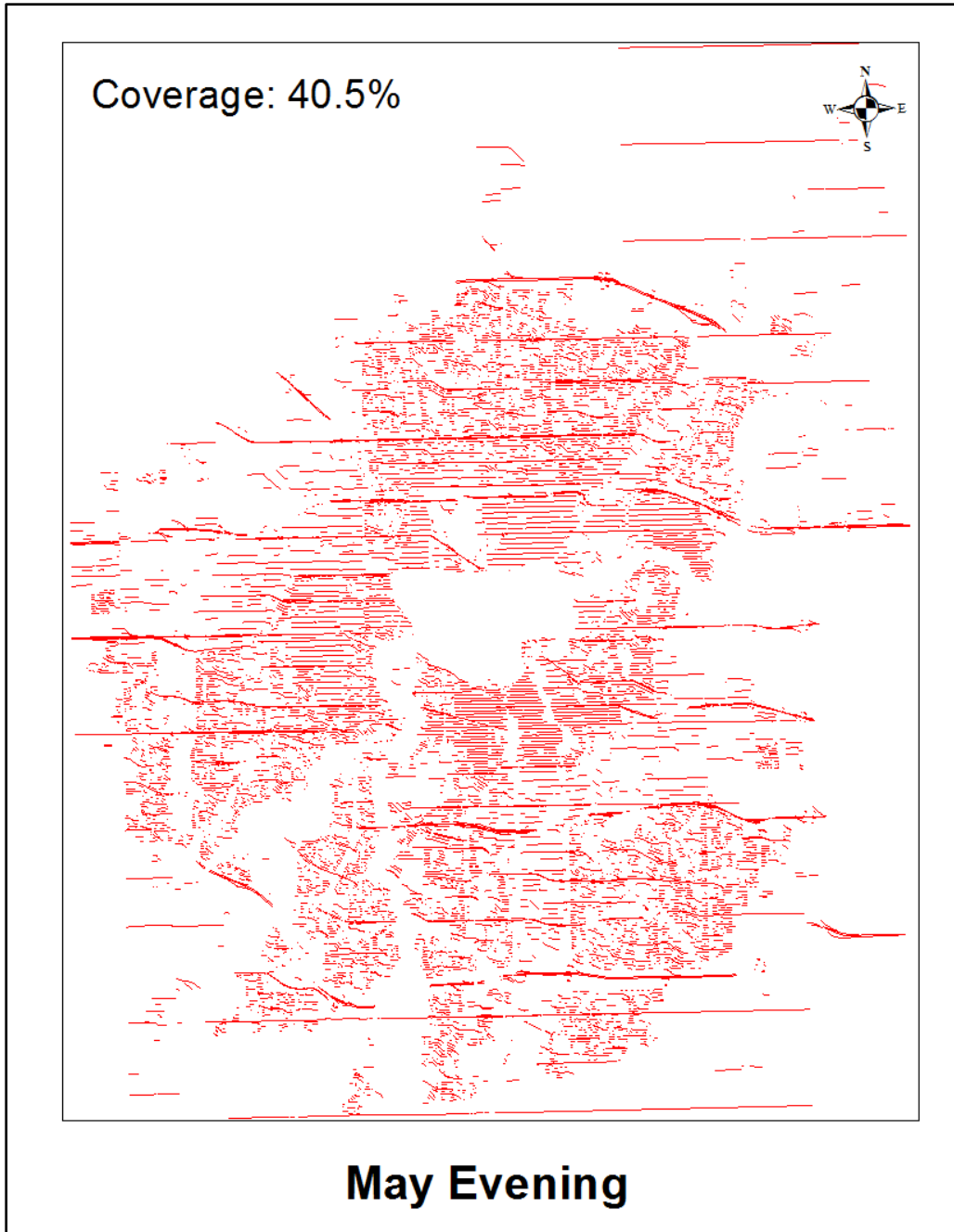
Figure B. 5 Glare prone locations of morning glare period in May
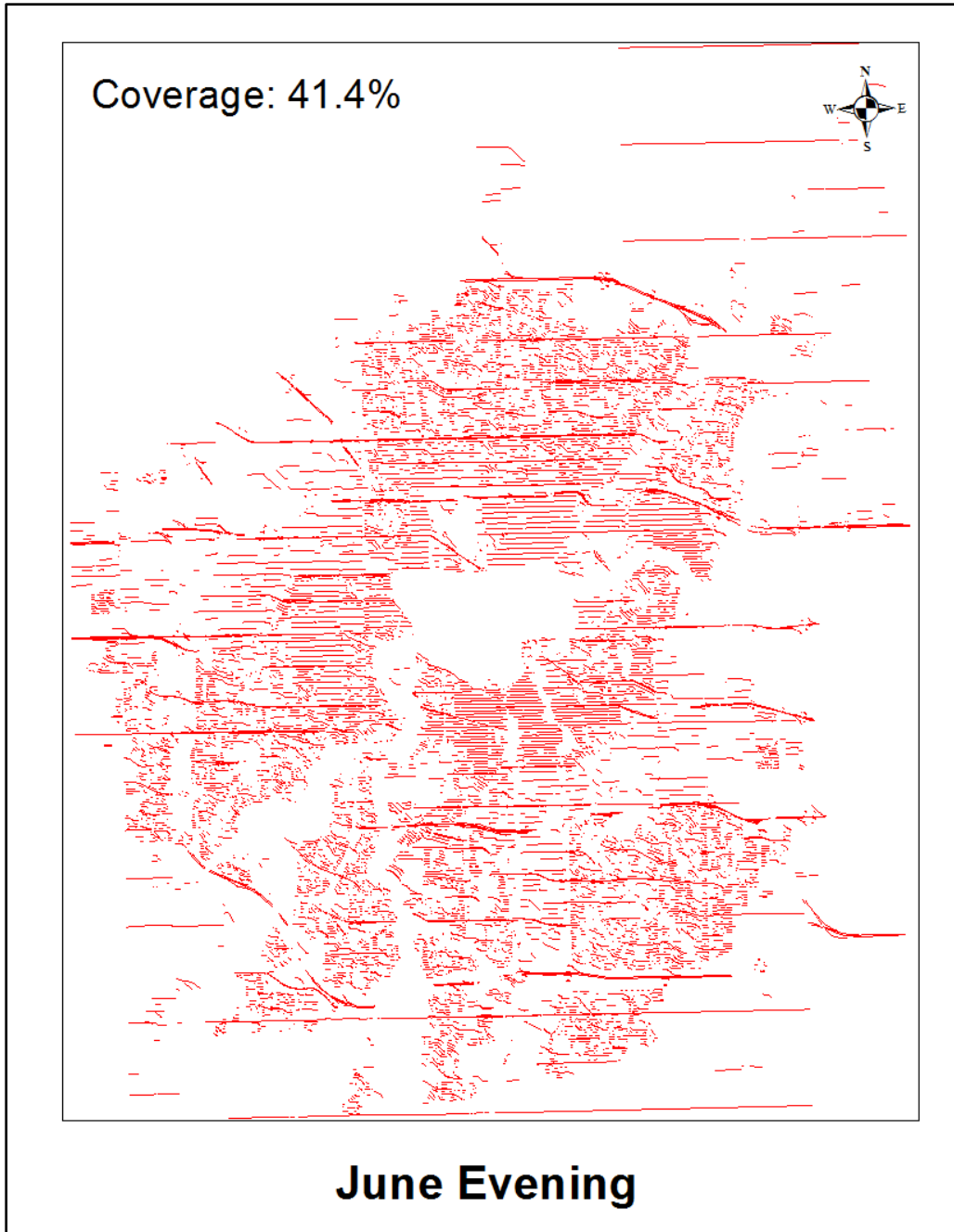
Figure B. 6 Glare prone locations of morning glare period in June
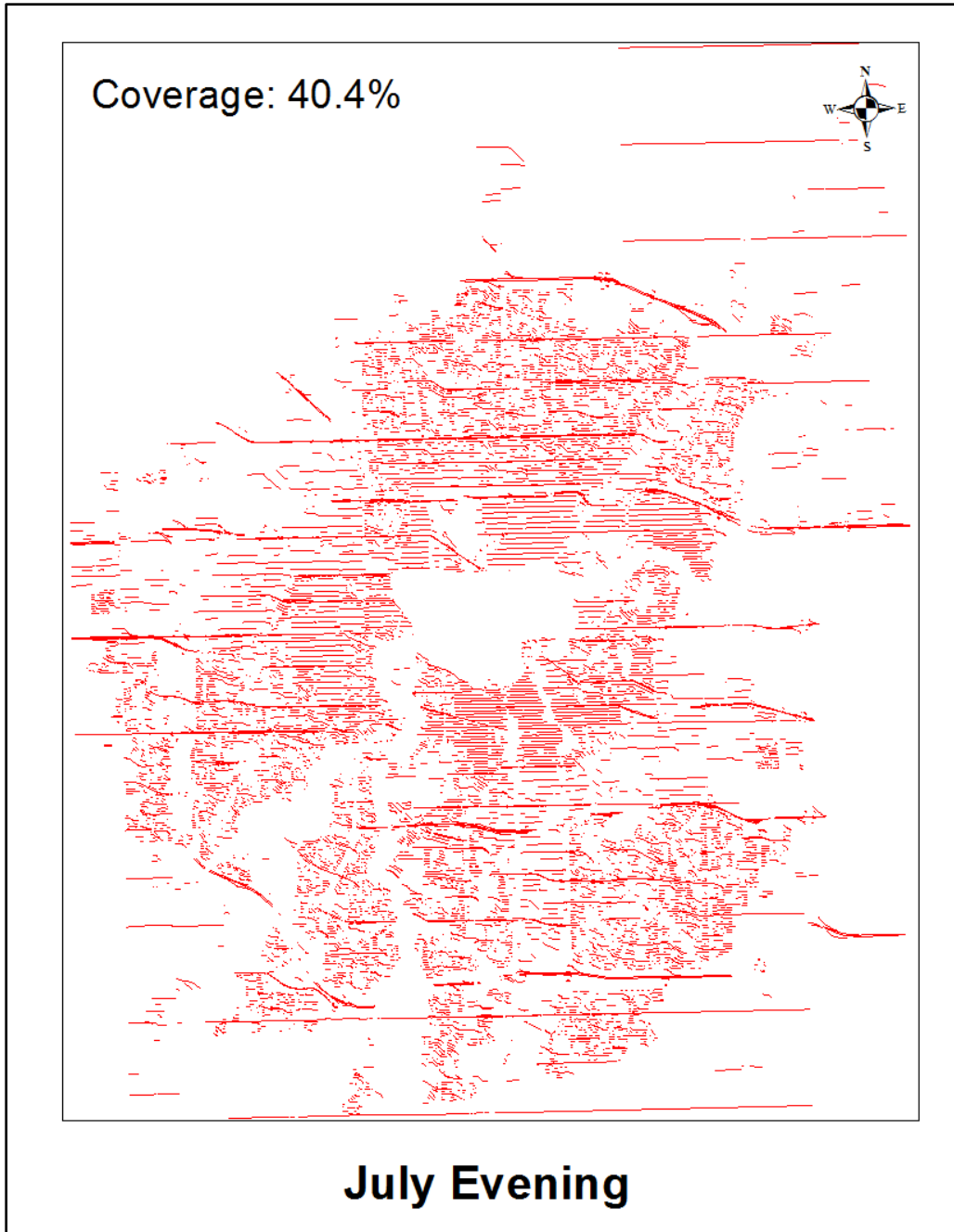
Figure B. 7 Glare prone locations of morning glare period in July

Coverage: 40.2%

August Evening

Figure B. 8 Glare prone locations of morning glare period in August

Figure B. 9 Glare prone locations of morning glare period in September
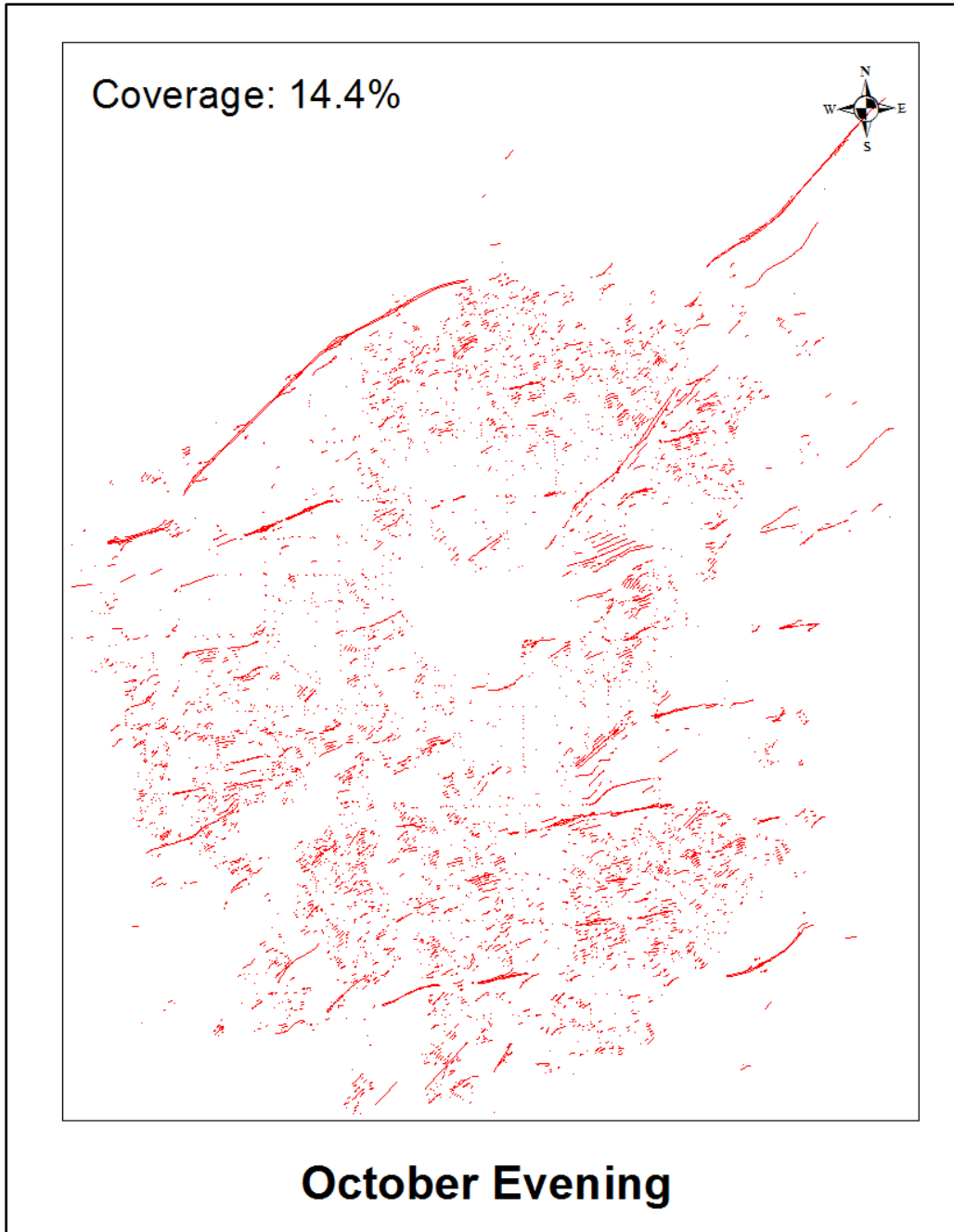
Figure B. 10 Glare prone locations of morning glare period in October

APPENDIX C. GLARE PRONE LOCATIONS OF ALL DAYTIME GLARE
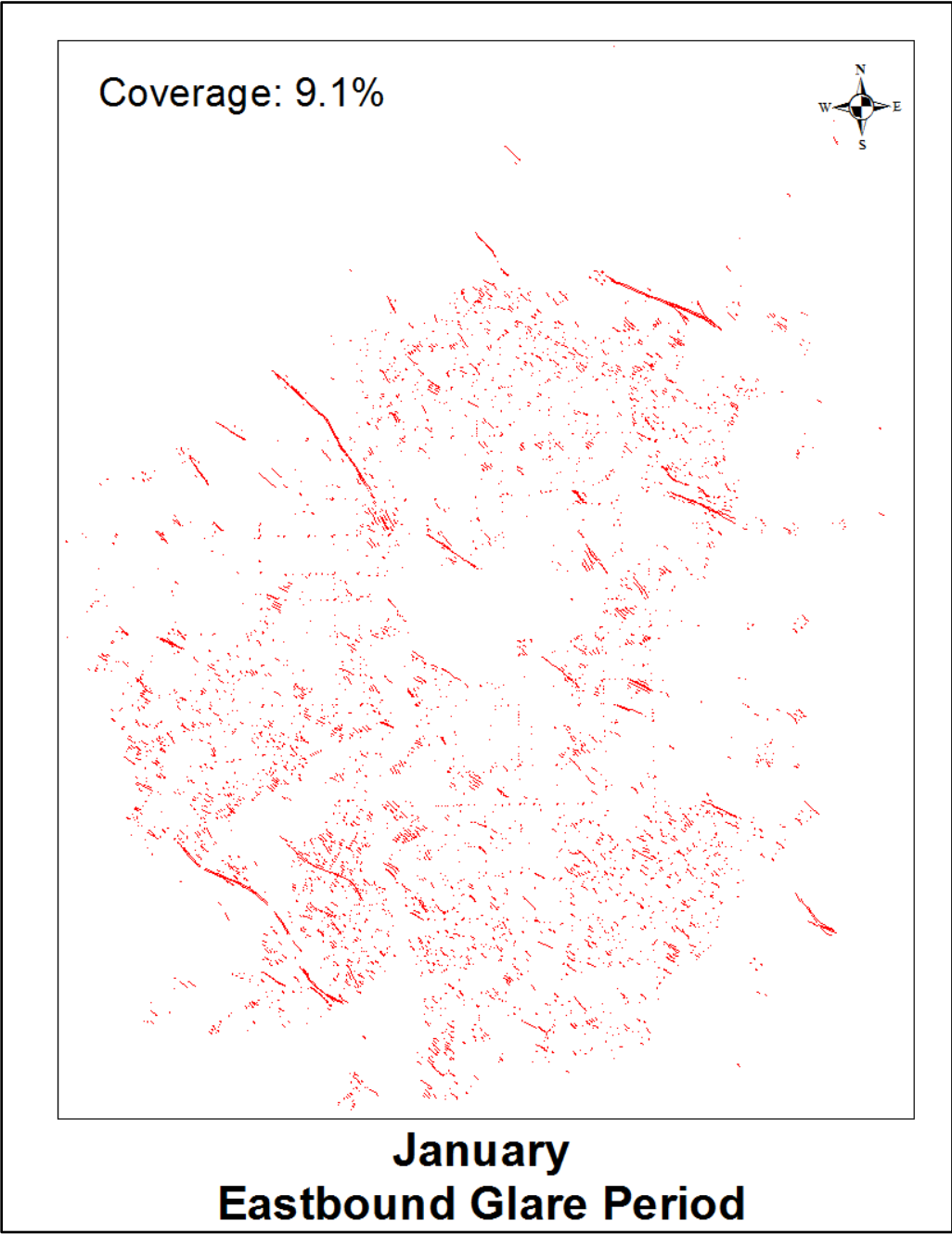
Figure C. 1 Glare prone locations of eastbound glare period in January

Coverage: 54.1%

January
Southbound Glare Period
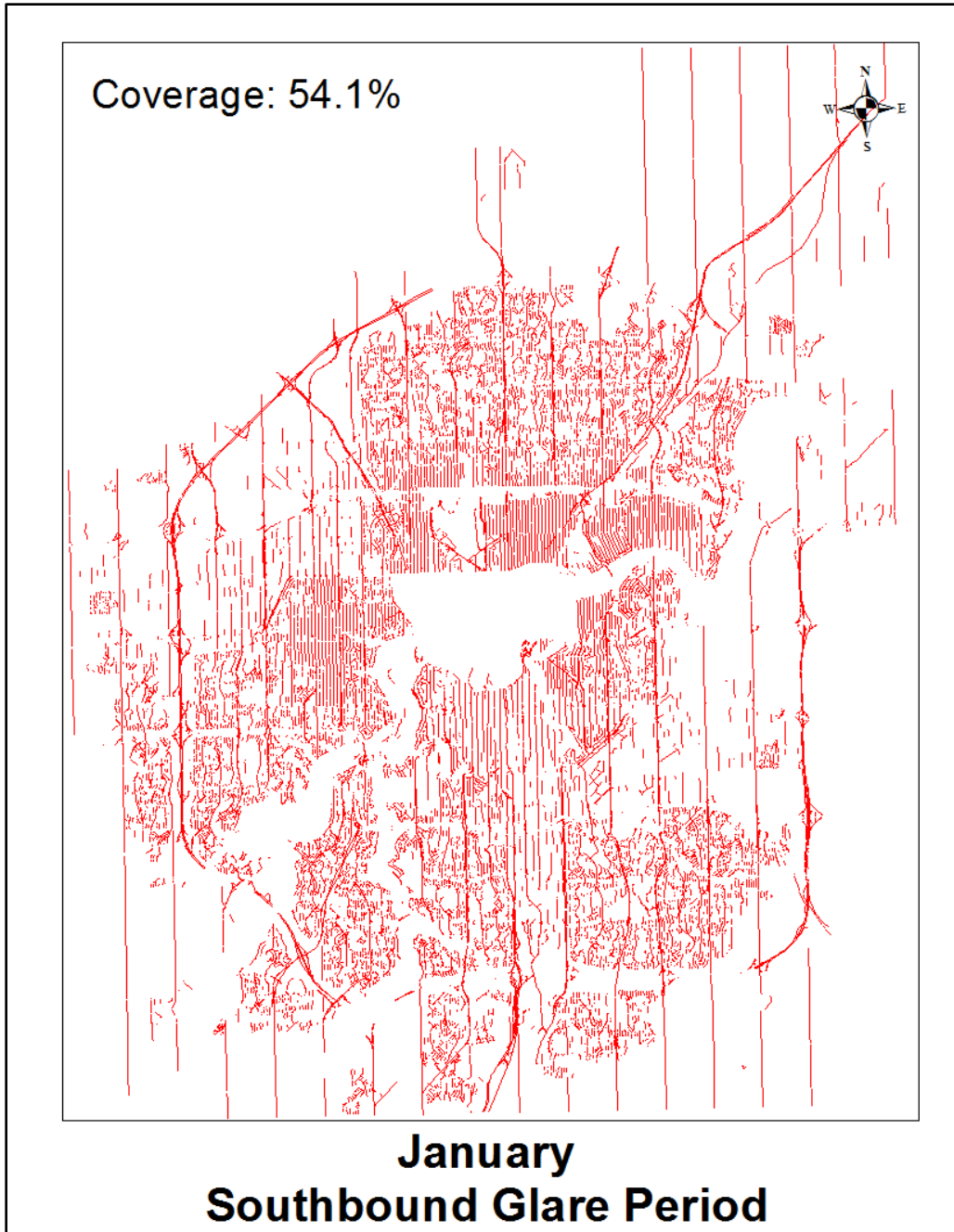
Figure C. 2 Glare prone locations of southbound glare period in January
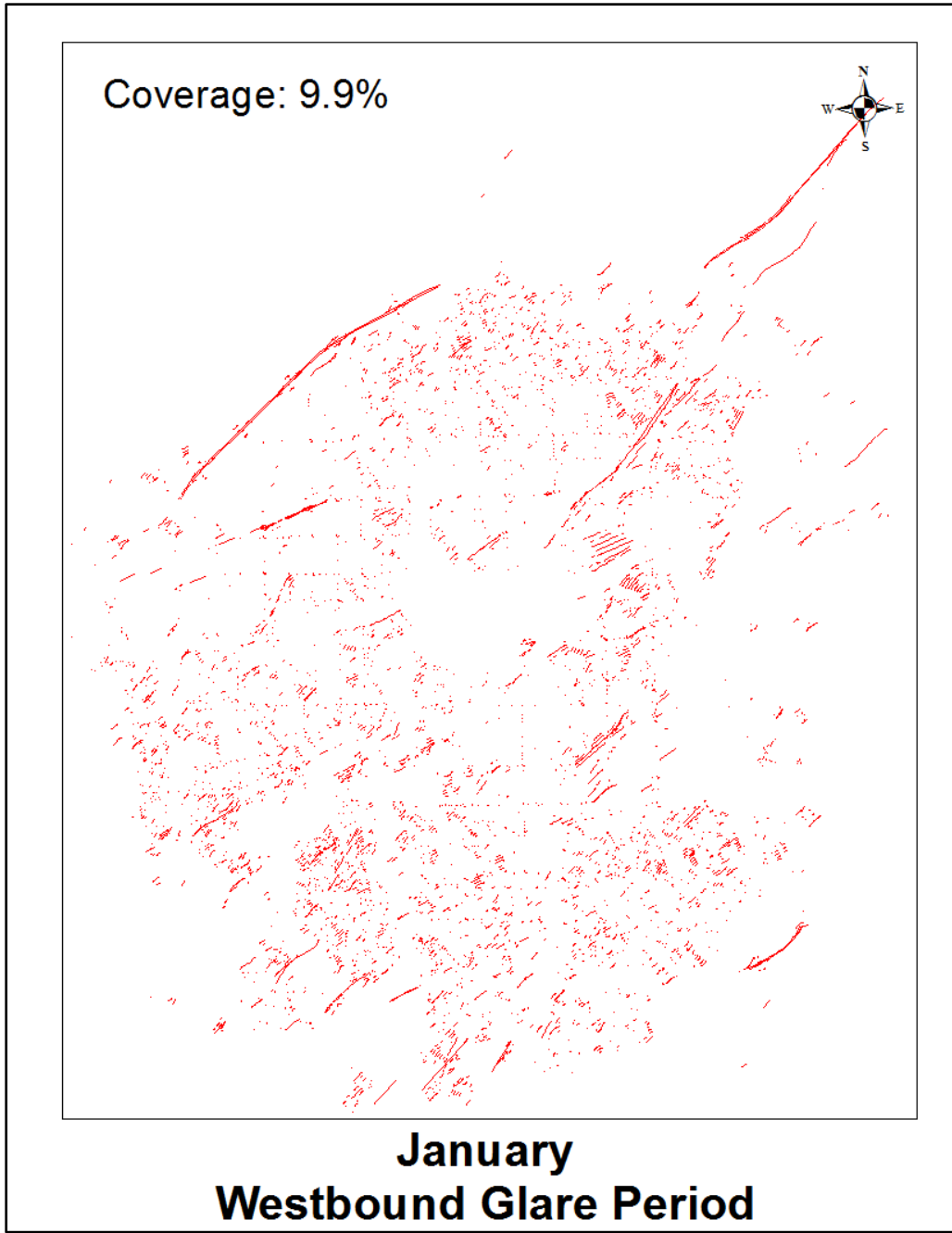
Figure C. 3 Glare prone locations of westbound glare period in January
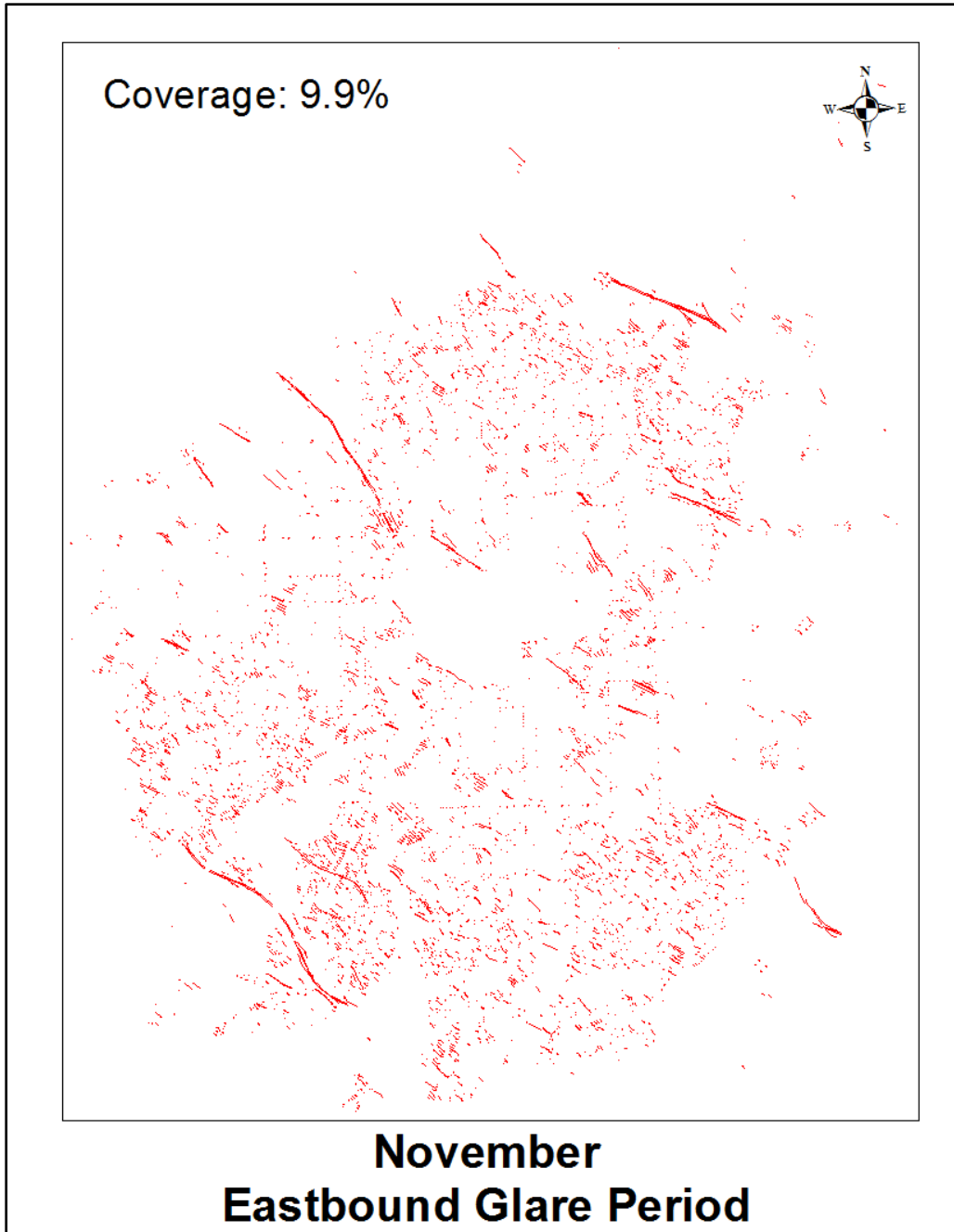
**Figure C. 4 Glare prone locations of eastbound glare period in November**
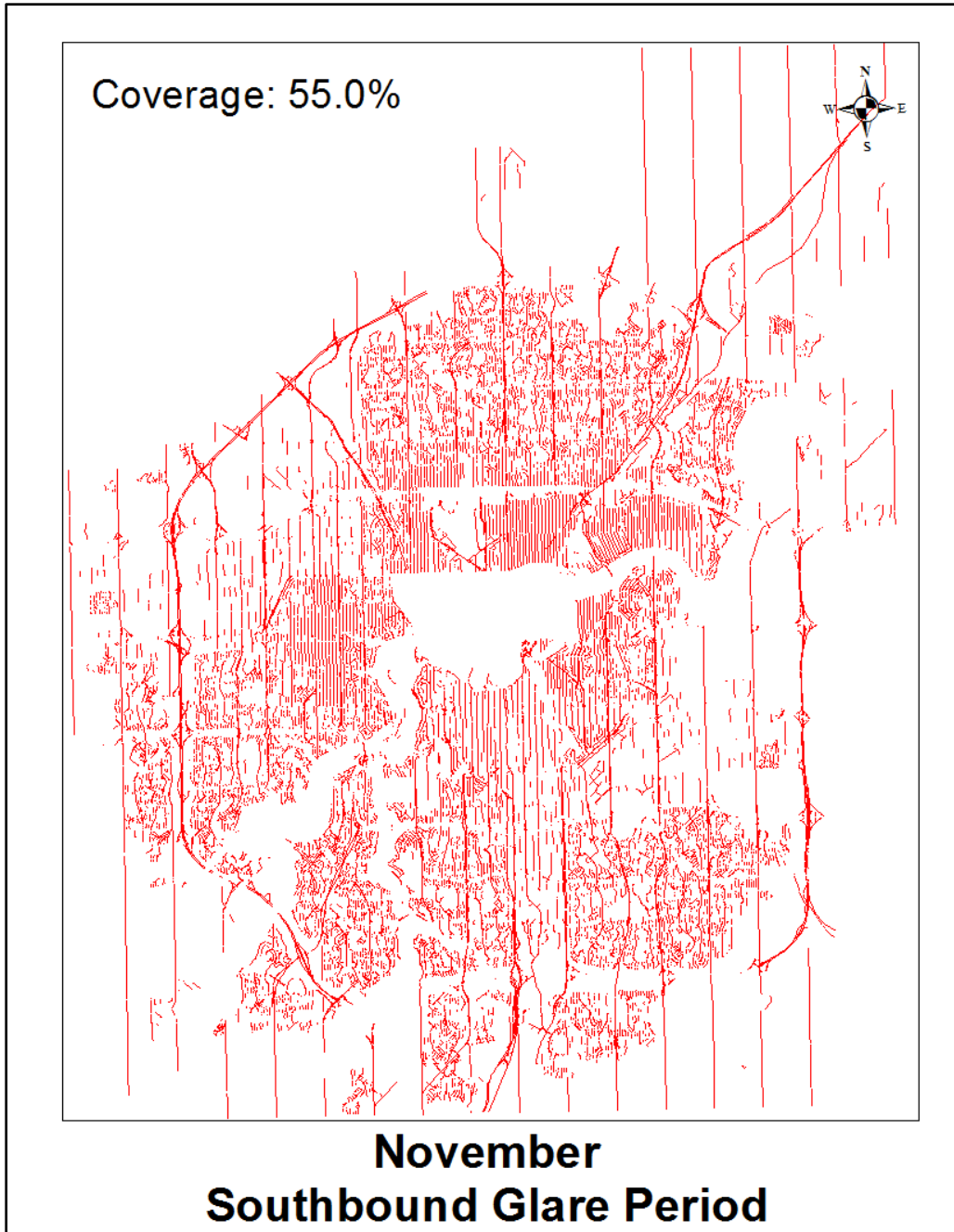
Figure C. 5 Glare prone locations of southbound glare period in November
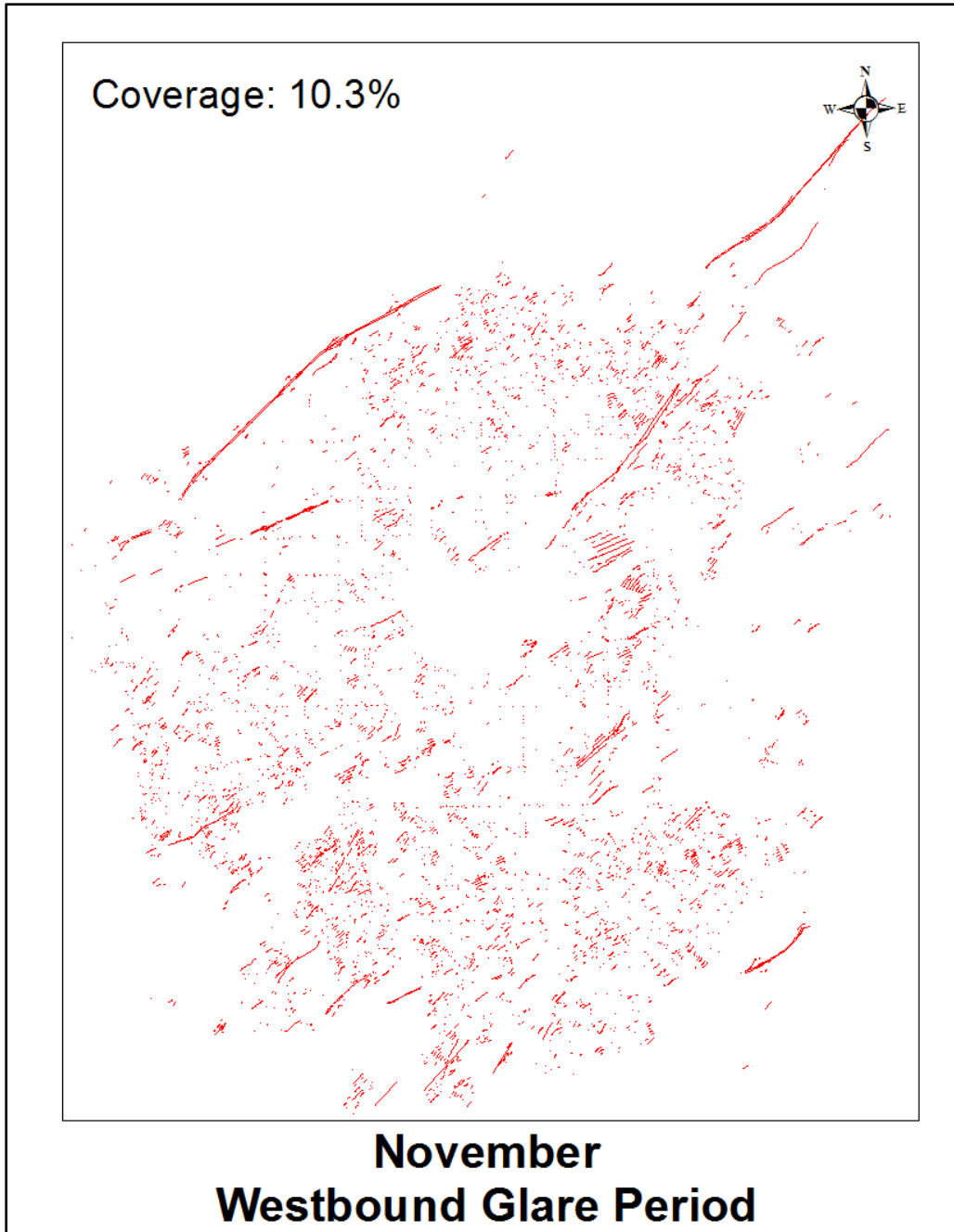
**Figure C. 6 Glare prone locations of westbound glare period in November**

Coverage: 56.8%

December
Southbound Glare Period
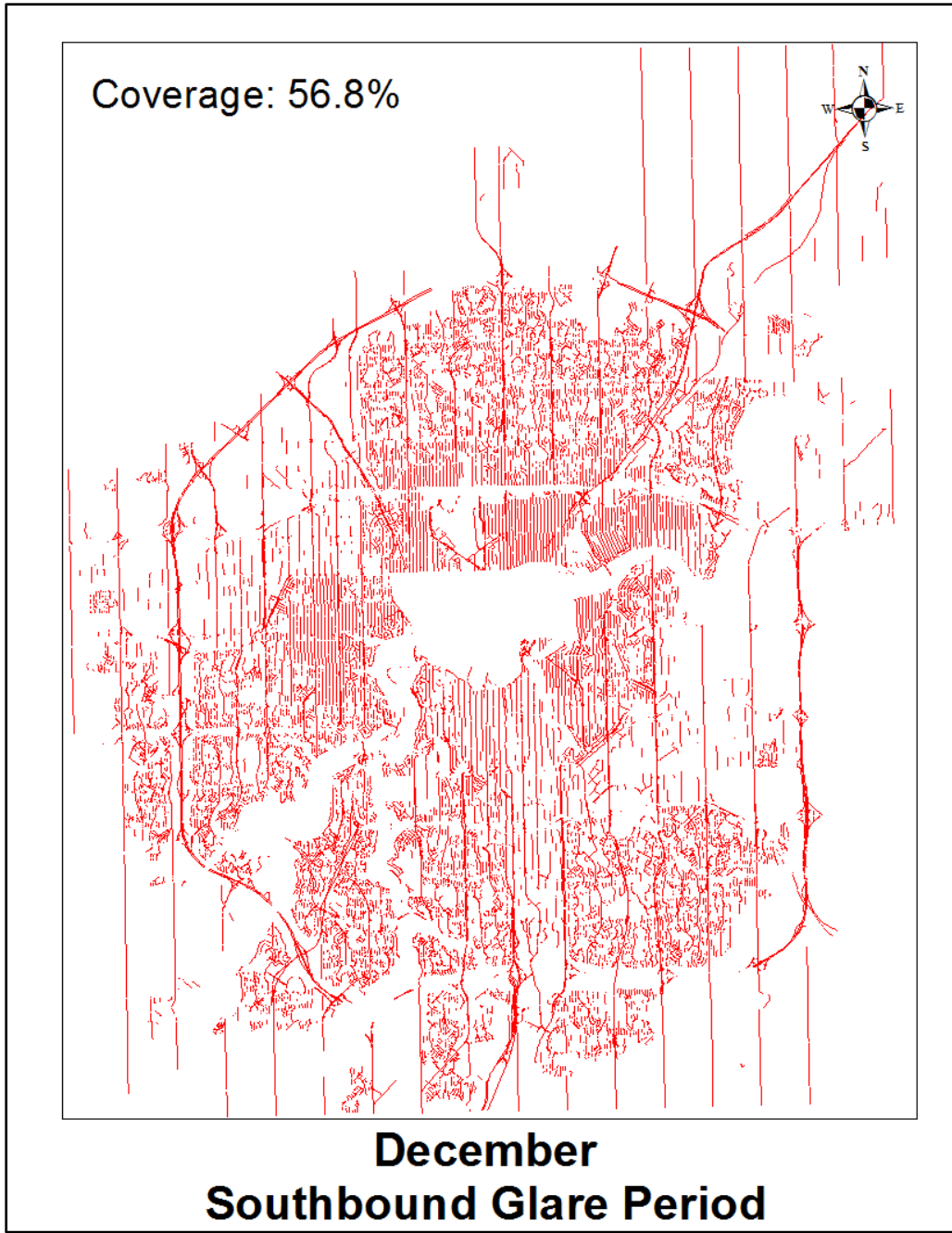
Figure C. 7 Glare prone locations of southbound glare period in December

APPENDIX D. COMPLETE RESUTS OF THE WILCOXON SIGNED-RANK TEST

Table D.1 Complete results of the Wilcoxon Signed-Rank Test for intersection collisions

Glare period	Pair i	Month	Glare Collision Ratio		$X_{Ai} - X_{Bi}$			$sign * R_i$
			Case Group X_{Ai}	Control Group X_{Bi}	sign	abs	R_i	
Morning	1	Feb	0.39	0.39	1	0.00	-	0
	2	Mar	0.54	0.47	1	0.07	8	8
	3	Apr	0.37	0.39	-1	0.02	2	-2
	4	May	0.46	0.24	1	0.22	16	16
	5	Jun	0.47	0.30	1	0.17	14	14
	6	Jul	0.39	0.30	1	0.09	10	10
	7	Aug	0.45	0.28	1	0.17	12	12
	8	Sep	0.43	0.26	1	0.18	15	15
	9	Oct	0.26	0.23	1	0.03	5	5
Evening	10	Feb	0.33	0.27	1	0.05	7	7
	11	Mar	0.37	0.20	1	0.17	13	13
	12	Apr	0.42	0.35	1	0.08	9	9
	13	May	0.29	0.18	1	0.11	11	11
	14	Jun	0.26	0.25	1	0.01	1	1
	15	Jul	0.33	0.36	-1	0.03	4	-4
	16	Aug	0.31	0.35	-1	0.04	6	-6
	17	Sep	0.53	0.28	1	0.25	17	17
	18	Oct	0.20	0.22	-1	0.02	3	-3
						W statistic		123
						Z		2.91

Table D.2 Complete results of the Wilcoxon Signed-Rank Test for mid-block collisions

Glare period	Pair i	Month	Glare Collision Ratio		$X_{Ai} - X_{Bi}$			$sign * R_i$
			Case Group X_{Ai}	Control Group X_{Bi}	sign	abs	R_i	
Morning	1	Feb	2.00	2.50	-1	0.50	12	-12
	2	Mar	1.85	0.77	1	1.08	17	17
	3	Apr	2.00	1.61	1	0.39	9	9
	4	May	1.23	0.81	1	0.42	10	10
	5	Jun	0.68	0.50	1	0.18	5	5
	6	Jul	0.75	1.50	-1	0.75	16	-16
	7	Aug	1.11	0.58	1	0.53	13	13
	8	Sep	1.41	0.85	1	0.57	14	14
	9	Oct	0.50	0.86	-1	0.36	8	-8
Evening	10	Feb	1.09	1.22	-1	0.13	2	-2
	11	Mar	0.58	0.75	-1	0.17	4	-4
	12	Apr	0.75	0.73	1	0.02	1	1
	13	May	1.00	0.80	1	0.20	6	6
	14	Jun	0.57	1.29	-1	0.71	15	-15
	15	Jul	1.50	0.41	1	1.09	18	18
	16	Aug	0.64	1.07	-1	0.42	11	-11
	17	Sep	1.24	0.92	1	0.32	7	7
	18	Oct	0.92	0.77	1	0.15	3	3
						W statistic		35
						Z		0.76